fractal and fractional

Article

Adaptive Quantized Synchronization of Fractional-Order Output-Coupling Multiplex Networks

Yunzhan Bai, Juan Yu * and Cheng Hu

College of Mathematics and System Science, Xinjiang University, Urumqi 830017, China
* Correspondence: yujuanseesea@163.com

Abstract: This paper is devoted to investigating the synchronization of fractional-order output-coupling multiplex networks (FOOCMNs). Firstly, a type of fractional-order multiplex network is introduced, where the intra-layer coupling and the inter-layer coupling are described separately, and nodes communicate with each other by their outputs, which is more realistic when the node states are unmeasured. By using the Lyapunov method and the fractional differential inequality, sufficient conditions are provided for achieving asymptotic synchronization based on the designed adaptive control, where the synchronized state of each layer is different. Furthermore, a quantized adaptive controller is developed to realize the synchronization of FOOCMNs, which effectively reduces signal transmission frequency and improves the effective utilization rate of network resources. Two numerical examples are given at last to support the theoretical analysis.

Keywords: fractional order; output coupling; multiplex network; quantized control; adaptive synchronization

MSC: 34A08; 93D20; 37N35

check for updates

Citation: Bai, Y.; Yu, J.; Hu, C. Adaptive Quantized Synchronization of Fractional-Order Output-Coupling Multiplex Networks. *Fractal Fract.* **2023**, *7*, 22. https://doi.org/10.3390/fractalfract7010022

Academic Editors: António Lopes, Zhouchao Wei and Lulu Lu

Received: 11 November 2022
Revised: 20 December 2022
Accepted: 21 December 2022
Published: 26 December 2022

1. Introduction

Complex networks can be traced back to Euler's pioneering graph theory, which can be used to describe a large number of complex dynamical systems in the real world, such as the Internet [1], biology [2], and the World Wide Web [3]. With the development of complex networks, single-layer networks can no longer meet the requirements of the existing complex systems, and research on multi-layer networks is urgently needed. According to the different connection types among layers, multi-layer networks can be divided into multiplex networks [4,5], multilayer networks [6,7], networks of networks [8], hyper networks [9], and interconnected network [10]. Among them, multiplex networks have a wide range of applications in various real fields, including social networks [11], transportation networks [12], and biological networks [13]. Nowadays, multiplex networks have become one of the important research directions in the field of complex networks.

On the other hand, fractional calculus refers to the differential and integral of any order, which can be regarded as the extension of the integral calculus, and has been widely used in physics, engineering, and other fields [14,15]. Compared with integer calculus, fractional calculus is more suitable for describing the change process with memory and hereditary characteristics. Therefore, it is closer to reality, and it is more complete to construct a dynamic model by means of a fractional differential equation. It is worth noting that although scholars have conducted a large number of studies on the dynamic characteristics of fractional-order complex networks [16–20], there are few studies on fractional-order multiplex networks [21]. Hence, it is necessary to study the dynamic behavior of fractional-order multiplex networks.

The synchronization phenomenon is widespread in real life, and the synchronization of complex networks refers to the collective dynamic behaviour of the various nodes in the network under certain conditions, which plays a significant role in intelligent optimization, secure communication, signal recognition, and other fields [22]. State-based coupling and output-based coupling are two common communication modes in complex networks, and most of the existing literature has focused on node state coupling [16–21]. However, the state-coupled network needs to transmit the state information of all nodes, which will cause the channel resources to be tight. On the other hand, the node states are not always measured due to environmental interference and physical and economic constraints. Therefore, it is necessary to study the synchronization of output-coupling complex networks.

Nowadays, many various control strategies have been developed, including adaptive control [23], intermittent control [24], pulse control [25], and event-triggered control [26]. Usually, the control gain is selected as a constant, but its value is often greater than the actual need. Fortunately, adaptive control can perfectly address this trouble, where the control gain varies and can be automatically adjusted over time. Contrary to rich results on adaptive control for integer-order complex networks, little attention has been paid to the adaptive synchronization of fractional-order multiplex networks. Very recently, Lv et al. in [27] studied the adaptive synchronization of fractional-order coupled neural networks with reaction-diffusion terms. Yang et al. in [28] developed a rigorous analytic tool for the adaptive control of fractional-order models. In [29], Liu et al. designed a new effective adaptive control to investigate the synchronization of fractional-order multiple neural networks. Compared with the traditional adaptive control, it not only removes the linear term, but also has the advantages of pinning control and adaptive control. Luo et al. in [30] analyzed the adaptive synchronization of multiplex networks with fractional order and time delays by the Lyapunov method and a new Halanay-type fractional inequality.

In addition, transmitted signals are often inevitably lost due to limitations and interference. Luckily, signal quantization was proposed by Kalman [31], which can reduce the bandwidth pressure and the risk of data loss. From then on, the quantitative control of complex networks has attracted extensive attention. For example, Wu et al. used the quantized control strategy to research the bounded consensus problem of multi-agents in [32]. Sun et al. in [33] discussed the synchronization of discrete-time neural networks by using a quantized sliding mode control. Combining an adaptive technique with quantized output control, Bao et al. discussed the synchronization of fractional-order coupled neural networks by the Lyapunov approach and LMIs technique in [34].

From the aforementioned analysis, the present work mainly focuses on the synchronization of multiplex networks with the first-order, which is extremely lacking for fractional-order multiplex networks. In particular, it is still an open and challenging problem for fractional-order multiplex networks to develop adaptive quantized control for the realization of synchronization. In addition, the state coupling is only considered in the most of the studies on multiplex networks, but it is invalid when the nodes' states are not measured. Therefore, it is popular and valuable to develop a coupling mode based on output states obtained by observation. Inspired by this, the main purpose of this article is to deal with the synchronization of FOOCMNs based on adaptive quantization control. The main contributions of this article are listed below.

(1) Different from the models of multiplex networks [35,36], the intra-layer coupling and the inter-layer coupling are described separately in the modelling of multiplex networks in this article. In addition, instead of the state coupling in [29,30,37], nodes communicate with each other by their output states, which is more realistic and valuable when the node states are unmeasured.
(2) Quantized adaptive control is introduced to achieve the synchronization of fractional-order multiplex networks for the first time, which can reduce signal transmission frequency and improve the effective utilization rate of network resources compared with the traditional adaptive control utilized in [27–30].
(3) The developed control schemes and the synchronization criteria are more generic, since they are also applicable when the factional-order system is reduced to the integer-

order model. Thus, our results can be regarded as a valuable extension of the previous results on the integer-order multiplex networks [35–37].

The remainder of this article is described below. Some basic preliminaries together with model descriptions are introduced in Section 2. Some criteria are established in Section 3 to synchronize multiplex networks. In Section 4, two numerical examples are provided to illustrate the proposed model and synchronization results. The summary of this article is given in Section 5.

Notation 1. *Throughout this article,* $\mathbb{R} = (-\infty, +\infty)$ *and* $\mathbb{R}^n$ *denote the n-dimensional Euclidean space. T represents the transposition of a matrix or a vector.* I_n *is the* $n \times n$ *identity matrix.* $\tilde{\mathfrak{N}} = \{1, 2, \ldots, \mathfrak{N}\}$ *and* $\tilde{\mathfrak{M}} = \{1, 2, \ldots, \mathfrak{M}\}$*.* $\|\cdot\|$ *is the Euclidean norm in* $\mathbb{R}^n$*. For a matrix* $\mathfrak{A} \in \mathbb{R}^{n\times n}$*,* $\mathfrak{A} > 0$ *represents that* $\mathfrak{A}$ *is positive definite, and* $\lambda_{\max}(\mathfrak{A})$ *and* $\lambda_{\min}(\mathfrak{A})$ *are the largest and smallest eigenvalues of the matrix* $\mathfrak{A}$ *when it is symmetric.* $\otimes$ *denotes the Kronecker product.*

2. Preliminaries and Model Description

2.1. Preliminaries

Definition 1 ([38])**.** *Function* $\bar{\phi}(t) : [t_0, +\infty) \to \mathbb{R}$ *is integrable. The fractional-order integral is defined as*

$$ {}_{t_0}I_t^{\bar{\alpha}}\bar{\phi}(t) = \frac{1}{\Gamma(\bar{\alpha})}\int_{t_0}^{t} \frac{\bar{\phi}(s)}{(t-s)^{1-\bar{\alpha}}} ds, \quad 0 < \bar{\alpha} < 1, $$

where $\Gamma(\bar{\alpha}) = \int_0^{+\infty} t^{\bar{\alpha}-1}e^{-t}dt$*.*

Definition 2 ([38])**.** *Function* $\bar{\phi}(t) : [t_0, +\infty) \to \mathbb{R}$ *is differentiable. The Caputo fractional-order derivative is defined by*

$$ {}_{t_0}^{C}D_t^{\bar{\alpha}}\bar{\phi}(t) = \frac{1}{\Gamma(1-\bar{\alpha})}\int_{t_0}^{t} \frac{\bar{\phi}'(s)}{(t-s)^{\bar{\alpha}}} ds, \quad 0 < \bar{\alpha} < 1. $$

Definition 3 ([38])**.** *Let* $\bar{\alpha}, \bar{\beta} > 0$*. The Mittag–Leffler function* $E_{\bar{\alpha},\bar{\beta}}$ *is defined by*

$$ E_{\bar{\alpha},\bar{\beta}}(z) = \sum_{k=0}^{+\infty} \frac{z^k}{\Gamma(\bar{\alpha}k + \bar{\beta})}. $$

When $\bar{\beta} = 1$*, the one-parameter form of it is defined by*

$$ E_{\bar{\alpha}}(z) = \sum_{k=0}^{+\infty} \frac{z^k}{\Gamma(\bar{\alpha}k + 1)}. $$

Lemma 1 ([38])**.** *If function* $\bar{\phi}(t) : [t_0, +\infty) \to \mathbb{R}$ *is continuously differentiable, then*

$$ {}_{t_0}I_t^{\bar{\alpha}}\,{}_{t_0}^{C}D_t^{\bar{\alpha}}\bar{\phi}(t) = \bar{\phi}(t) - \bar{\phi}(t_0), \quad 0 < \bar{\alpha} < 1. $$

Lemma 2 ([39])**.** *Assume that* $\bar{\psi}(t) \in \mathbb{R}$ *is continuously differentiable; then, for any* $t \geq t_0$*,*

$$ \frac{1}{2}\,{}_{t_0}^{C}D_t^{\bar{\alpha}}\bar{\psi}^2(t) \leq \bar{\psi}(t)\,{}_{t_0}^{C}D_t^{\bar{\alpha}}\bar{\psi}(t), \quad 0 < \bar{\alpha} < 1. $$

In addition, when $\bar{\psi}(t) \in \mathbb{R}^n$*, then for any* $t \geq t_0$*,*

$$ \frac{1}{2}\,{}_{t_0}^{C}D_t^{\bar{\alpha}}\bar{\psi}^T(t)\bar{\psi}(t) \leq \bar{\psi}^T(t)\,{}_{t_0}^{C}D_t^{\bar{\alpha}}\bar{\psi}(t), \quad 0 < \bar{\alpha} < 1. $$

2.2. Model Description

This article will investigate a type of FOOCMN, which has $\mathfrak{M}$ layers and $\mathfrak{N}$ nodes in each layer. Let $\mathcal{T}^{\kappa} = \{\mathcal{V}, \varepsilon^{\kappa}, G^{\kappa}\}$ be a undirected graph corresponding to the κth layer with the node set $\mathcal{V} = \{1, 2, \ldots, \mathfrak{N}\}$, the edge set $\varepsilon^{\kappa} \subseteq \mathcal{V} \times \mathcal{V}$, and the adjacency matrix $G^{\kappa} = \left(G^{\kappa}_{\imath\jmath}\right)_{\mathfrak{N}\times\mathfrak{N}}$. Here, $G^{\kappa}_{\imath\jmath} > 0$ if the $\imath$th node and the $\jmath$th node are communicated at the κth layer; otherwise, the value of it is 0.

The dynamics of FOOCMN are depicted as the following differential model:

$$\begin{cases} {}^{C}_{t_0}D^{\bar{\alpha}}_{t} x^{(\kappa)}_{\imath}(t) = \bar{f}(x^{(\kappa)}_{\imath}(t)) - \bar{a} \sum\limits_{\jmath=1}^{\mathfrak{N}} l^{(\kappa)}_{\imath\jmath} H z^{(\kappa)}_{\jmath}(t) - \bar{b} \sum\limits_{\bar{\iota}=1}^{\mathfrak{M}} d_{\kappa\bar{\iota}} P z^{(\bar{\iota})}_{\imath}(t) + u^{(\kappa)}_{\imath}(t), \\ z^{(\kappa)}_{\imath}(t) = \Gamma x^{(\kappa)}_{\imath}(t), \qquad \imath \in \tilde{N}, \kappa \in \tilde{M}, \end{cases} \tag{1}$$

where $0 < \bar{\alpha} < 1$, $x^{(\kappa)}_{\imath}(t) = \left(x^{(\kappa)}_{\imath 1}(t), x^{(\kappa)}_{\imath 2}(t), \ldots, x^{(\kappa)}_{\imath n}(t)\right)^{T} \in \mathbb{R}^{n}$ denotes the state of the $\imath$th node in the κth layer, $z^{(\kappa)}_{\imath}(t) = \left(z^{(\kappa)}_{\imath 1}(t), z^{(\kappa)}_{\imath 2}(t), \ldots, z^{(\kappa)}_{\imath m}(t)\right)^{T} \in \mathbb{R}^{m}$ is the output vector of the $\imath$th node, and $\bar{f}(\cdot) : \mathbb{R}^{n} \to \mathbb{R}^{n}$ is a smooth nonlinear vector function. $\bar{a}$ and $\bar{b}$ are the intra-layer and inter-layer coupling strengths, respectively. $H \in \mathbb{R}^{n\times m}$ represents an internal coupling matrix in each layer, $P \in \mathbb{R}^{n\times m}$ is an internal coupling matrix among nodes in the cross-layer, $\Gamma \in \mathbb{R}^{m\times n}$ is the output matrix, and $u^{(\kappa)}_{\imath}(t)$ denotes the adaptive feedback controller. $L^{(\kappa)} = (l^{(\kappa)}_{\imath\jmath})_{\mathfrak{N}\times\mathfrak{N}}$ denotes the Laplacian matrix of nodes in the κth layer, and $D = (d_{\kappa\bar{\iota}})_{\mathfrak{M}\times\mathfrak{M}}$ denotes the inter-layer Laplacian matrix. Elements $l^{(\kappa)}_{\imath\jmath}$ and $d_{\kappa\bar{\iota}}$ are defined as follows:

$$\begin{cases} l^{(\kappa)}_{\imath\jmath} = -1(\imath \neq \jmath), & \text{if the } \imath\text{th node is connected with the } \jmath\text{th node in the } \kappa\text{th layer}, \\ l^{(\kappa)}_{\imath\jmath} = 0(\imath \neq \jmath), & \text{otherwise}, \\ l^{(\kappa)}_{\imath\imath} = -\sum\limits_{\jmath=1,\jmath\neq\imath}^{N} l^{(\kappa)}_{\imath\jmath}, & \imath \in \tilde{\mathfrak{N}}, \kappa \in \tilde{\mathfrak{M}}, \end{cases}$$

$$\begin{cases} d_{\kappa\bar{\iota}} = -1(\kappa \neq \bar{\iota}), & \text{if the node in layer } \kappa \text{ is linked to its corresponding node in layer } \bar{\iota}, \\ d_{\kappa\bar{\iota}} = 0(\kappa \neq \bar{\iota}), & \text{otherwise}, \\ d_{\kappa\kappa} = -\sum\limits_{\bar{\iota}=1,\bar{\iota}\neq\kappa}^{M} d_{\kappa\bar{\iota}}, & \kappa \in \tilde{\mathfrak{M}}. \end{cases}$$

The target model of FOOCMN (1) is depicted as

$$\begin{cases} {}^{C}_{t_0}D^{\bar{\alpha}}_{t} s^{(\kappa)}(t) = \bar{f}(s^{(\kappa)}(t)), \\ y^{(\kappa)}(t) = \Gamma s^{(\kappa)}(t), \quad \kappa \in \tilde{\mathfrak{M}}, \end{cases} \tag{2}$$

where $s^{(\kappa)}(t) = (s^{(\kappa)}_{1}(t), s^{(\kappa)}_{2}(t), \cdots, s^{(\kappa)}_{n}(t))^{T} \in \mathbb{R}^{n}$ can be deemed as the synchronization state of the isolated node.

Let $e^{(\kappa)}_{\imath}(t) = x^{(\kappa)}_{\imath}(t) - s^{(\kappa)}(t)$ and $\theta^{(\kappa)}_{\imath}(t) = z^{(\kappa)}_{\imath}(t) - y^{(\kappa)}(t)$ be the synchronization error and output error. Tshe error model is governed as

$$\begin{cases} {}^{C}_{t_0}D^{\bar{\alpha}}_{t} e^{(\kappa)}_{\imath}(t) = \tilde{f}(e^{(\kappa)}_{\imath}(t)) - \bar{a} \sum\limits_{\jmath=1}^{\mathfrak{N}} l^{(\kappa)}_{\imath\jmath} H \theta^{(\kappa)}_{\jmath}(t) - \bar{b} \sum\limits_{\bar{\iota}=1}^{\mathfrak{M}} d_{\kappa\bar{\iota}} P \theta^{(\bar{\iota})}_{\imath}(t) + u^{(\kappa)}_{\imath}(t), \\ \theta^{(\kappa)}_{\imath}(t) = \Gamma e^{(\kappa)}_{\imath}(t), \quad \imath \in \tilde{\mathfrak{N}}, \kappa \in \tilde{\mathfrak{M}}, \end{cases} \tag{3}$$

where $\tilde{f}(e^{(\kappa)}_{\imath}(t)) = \bar{f}(x^{(\kappa)}_{\imath}(t)) - \bar{f}(s^{(\kappa)}(t))$.

Definition 4. *FOOCMN* (1) *is said to be asymptotically synchronized if*

$$\lim_{t\to+\infty} \left\| e^{(\kappa)}_{\imath}(t) \right\| = 0, \imath \in \tilde{\mathfrak{N}}, \kappa \in \tilde{\mathfrak{M}}.$$

Assumption 1. *For any $x_\imath, x_\jmath \in \mathbb{R}^n$, there exists a positive constant $\ell_{\bar{f}}$ such that*

$$\left\|\bar{f}(x_\imath) - \bar{f}(x_\jmath)\right\| \le \ell_{\bar{f}}\left\|x_\imath - x_\jmath\right\|, \quad \imath, \jmath \in \tilde{\mathfrak{N}}.$$

3. Main Results

In this section, some theorems and corollaries are proposed for the synchronization of FOOCMNs by the following controllers.

3.1. Adaptive Synchronization

Firstly, the adaptive controller $u_\imath^{(\kappa)}(t)$ is designed by

$$\begin{cases} u_\imath^{(\kappa)}(t) = -g_\imath^{(\kappa)}(t)\Gamma^T\theta_\imath^{(\kappa)}(t), \\ {}_{t_0}^{C}D_t^{\bar{\alpha}} g_\imath^{(\kappa)}(t) = \beta_\imath^{(\kappa)}\left\|\theta_\imath^{(\kappa)}(t)\right\|^2, \quad \imath \in \tilde{\mathfrak{N}}, \kappa \in \tilde{\mathfrak{M}}, \end{cases} \tag{4}$$

where $\beta_\imath^{(\kappa)} > 0$, $g_\imath^{(\kappa)}(0) \ge 0$.

Theorem 1. *Based on Assumption 1, FOOCMN (1) achieves asymptotic synchronization under Controller (4).*

Proof. Construct the following Lyapunov function

$$V(t) = \frac{1}{2}\sum_{\kappa=1}^{\mathfrak{M}}\sum_{\imath=1}^{\mathfrak{N}}(e_\imath^{(\kappa)}(t))^T e_\imath^{(\kappa)}(t) + \frac{1}{2}\sum_{\kappa=1}^{\mathfrak{M}}\sum_{\imath=1}^{\mathfrak{N}}\frac{1}{\beta_\imath^{(\kappa)}}\left(g_\imath^{(\kappa)}(t) - g^*\right)^2,$$

where g^* is an adaptive constant.

From Lemma 2, one obtains that

$$\begin{aligned}
{}_{t_0}^{C}D_t^{\bar{\alpha}} V(t) \le{}& \sum_{\kappa=1}^{\mathfrak{M}}\sum_{\imath=1}^{\mathfrak{N}}(e_\imath^{(\kappa)}(t))^T {}_{t_0}^{C}D_t^{\bar{\alpha}} e_\imath^{(\kappa)}(t) + \sum_{\kappa=1}^{\mathfrak{M}}\sum_{\imath=1}^{\mathfrak{N}}\frac{1}{\beta_\imath^{(\kappa)}}(g_\imath^{(\kappa)}(t) - g^*) {}_{t_0}^{C}D_t^{\bar{\alpha}} g_\imath^{(\kappa)}(t) \\
={}& \sum_{\kappa=1}^{\mathfrak{M}}\sum_{\imath=1}^{\mathfrak{N}}(e_\imath^{(\kappa)}(t))^T\Big[\tilde{f}(e_\imath^{(\kappa)}(t)) - \bar{a}\sum_{\jmath=1}^{\mathfrak{N}} l_{\imath\jmath}^{(\kappa)} H\theta_\jmath^{(\kappa)}(t) \\
&- \bar{b}\sum_{\bar{\iota}=1}^{\mathfrak{M}} d_{\kappa\bar{\iota}} P\theta_\imath^{(\bar{\iota})}(t) + u_\imath^{(\kappa)}(t)\Big] + \sum_{\kappa=1}^{\mathfrak{M}}\sum_{\imath=1}^{\mathfrak{N}}(g_\imath^{(\kappa)}(t) - g^*)\left\|\theta_\imath^{(\kappa)}(t)\right\|^2 \\
={}& \sum_{\kappa=1}^{\mathfrak{M}}\sum_{\imath=1}^{\mathfrak{N}}(e_\imath^{(\kappa)}(t))^T\tilde{f}(e_\imath^{(\kappa)}(t)) - \bar{a}\sum_{\kappa=1}^{\mathfrak{M}}\sum_{\imath=1}^{\mathfrak{N}}\sum_{\jmath=1}^{\mathfrak{N}}(e_\imath^{(\kappa)}(t))^T l_{\imath\jmath}^{(\kappa)} H\theta_\jmath^{(\kappa)}(t) \\
&- \bar{b}\sum_{\kappa=1}^{\mathfrak{M}}\sum_{\imath=1}^{\mathfrak{N}}\sum_{\bar{\iota}=1}^{\mathfrak{M}}(e_\imath^{(\kappa)}(t))^T d_{\kappa\bar{\iota}} P\theta_\imath^{(\bar{\iota})}(t) - \sum_{\kappa=1}^{\mathfrak{M}}\sum_{\imath=1}^{\mathfrak{N}}(e_\imath^{(\kappa)}(t))^T\Gamma^T g_\imath^{(\kappa)}(t)\theta_\imath^{(\kappa)}(t) \\
&+ \sum_{\kappa=1}^{\mathfrak{M}}\sum_{\imath=1}^{\mathfrak{N}}(g_\imath^{(\kappa)}(t) - g^*)\left\|\theta_\imath^{(\kappa)}(t)\right\|^2 \\
={}& \sum_{\kappa=1}^{\mathfrak{M}}\sum_{\imath=1}^{\mathfrak{N}}(e_\imath^{(\kappa)}(t))^T\tilde{f}(e_\imath^{(\kappa)}(t)) - \bar{a}\sum_{\kappa=1}^{\mathfrak{M}}\sum_{\imath=1}^{\mathfrak{N}}\sum_{\jmath=1}^{\mathfrak{N}}(e_\imath^{(\kappa)}(t))^T l_{\imath\jmath}^{(\kappa)} H\theta_\jmath^{(\kappa)}(t) \\
&- \bar{b}\sum_{\kappa=1}^{\mathfrak{M}}\sum_{\imath=1}^{\mathfrak{N}}\sum_{\bar{\iota}=1}^{\mathfrak{M}}(e_\imath^{(\kappa)}(t))^T d_{\kappa\bar{\iota}} P\theta_\imath^{(\bar{\iota})}(t) - \sum_{\kappa=1}^{\mathfrak{M}}\sum_{\imath=1}^{\mathfrak{N}} g^*\left\|\theta_\imath^{(\kappa)}(t)\right\|^2.
\end{aligned} \tag{5}$$

According to Assumption 1, one obtains

$$\begin{aligned}&\sum_{\kappa=1}^{\mathfrak{M}}\sum_{\imath=1}^{\mathfrak{N}}(e_\imath^{(\kappa)}(t))^T\tilde{f}(e_\imath^{(\kappa)}(t))\\&\leq\sum_{\kappa=1}^{\mathfrak{M}}\sum_{\imath=1}^{\mathfrak{N}}\ell_f e_\imath^{(\kappa)}(t)^T e_\imath^{(\kappa)}(t).\end{aligned}\tag{6}$$

By defining

$$e^{(\kappa)}(t)=(e_1^{(\kappa)}(t)^T,e_2^{(\kappa)}(t)^T\ldots,e_{\mathfrak{N}}^{(\kappa)}(t)^T)^T,e(t)=(e^{(1)}(t)^T,e^{(2)}(t)^T,\ldots,e^{(\mathfrak{M})}(t)^T)^T,$$

$$e_\imath(t)=(e_\imath^{(1)}(t)^T,e_\imath^{(2)}(t)^T\ldots,e_\imath^{(\mathfrak{M})}(t)^T)^T,\tilde{e}(t)=(e_1(t)^T,e_2(t)^T,\ldots,e_{\mathfrak{N}}(t)^T)^T,$$

it follows that

$$\begin{aligned}&-\bar{a}\sum_{\kappa=1}^{\mathfrak{M}}\sum_{\imath=1}^{\mathfrak{N}}\sum_{\jmath=1}^{\mathfrak{N}}(e_\imath^{(\kappa)}(t))^T l_{\imath\jmath}^{(\kappa)}H\theta_\jmath^{(\kappa)}(t)\\&=-\bar{a}\sum_{\kappa=1}^{\mathfrak{M}}\sum_{\imath=1}^{\mathfrak{N}}\sum_{\jmath=1}^{\mathfrak{N}}(e_\imath^{(\kappa)}(t))^T l_{\imath\jmath}^{(\kappa)}H\Gamma e_\jmath^{(\kappa)}(t)\\&=-\bar{a}\sum_{\kappa=1}^{\mathfrak{M}}\left[(e^{(\kappa)}(t))^T(L^{(\kappa)}\otimes(H\Gamma))e^{(\kappa)}(t)\right]\\&=\bar{a}e^T(t)(-L\otimes(\frac{H\Gamma+(H\Gamma)^T}{2}))e(t)\\&\leq\bar{a}\lambda_1\|e(t)\|^2,\end{aligned}\tag{7}$$

and

$$\begin{aligned}&-\bar{b}\sum_{\kappa=1}^{\mathfrak{M}}\sum_{\imath=1}^{\mathfrak{N}}\sum_{\bar{\imath}=1}^{\mathfrak{M}}(e_\imath^{(\kappa)}(t))^T d_{\kappa\bar{\imath}}P\theta_\imath^{(\bar{\imath})}(t)\\&=-\bar{b}\sum_{\kappa=1}^{\mathfrak{M}}\sum_{\imath=1}^{\mathfrak{N}}\sum_{\bar{\imath}=1}^{\mathfrak{M}}(e_\imath^{(\kappa)}(t))^T d_{\kappa\bar{\imath}}P\Gamma e_i^{(\bar{\imath})}(t)\\&=\bar{b}\tilde{e}^T(t)(-I_{\mathfrak{N}}\otimes D\otimes(\frac{P\Gamma+(P\Gamma)^T}{2}))\tilde{e}(t)\\&\leq\bar{b}\lambda_2\|\tilde{e}(t)\|^2\\&=\bar{b}\lambda_2\|e(t)\|^2,\end{aligned}\tag{8}$$

where $L=diag(L^{(1)},L^{(2)},\ldots,L^{(\mathfrak{M})})$, $\lambda_1=\lambda_{\max}(-L\otimes(\frac{H\Gamma+(H\Gamma)^T}{2}))$ and $\lambda_2=\lambda_{\max}(-I_{\mathfrak{N}}\otimes D\otimes(\frac{P\Gamma+(P\Gamma)^T}{2}))$.

Substituting Inequalities (6)–(8) into (5), and choosing $g^*=\frac{\ell_f+\bar{a}\lambda_1+\bar{b}\lambda_2+1}{\lambda_3}$, it can be deduced that

$$\begin{aligned}{}_{t_0}^{C}D_t^{\bar{\alpha}}V(t)&\leq(\ell_f+\bar{a}\lambda_1+\bar{b}\lambda_2)\|e(t)\|^2-\sum_{\kappa=1}^{\mathfrak{M}}\sum_{\imath=1}^{\mathfrak{N}}g^*\left\|\theta_\imath^{(\kappa)}(t)\right\|^2\\&=(\ell_f+\bar{a}\lambda_1+\bar{b}\lambda_2)\|e(t)\|^2-g^*e^T(t)(I_{\mathfrak{M}\mathfrak{N}}\otimes(\Gamma^T\Gamma))e(t)\\&\leq(\ell_f+\bar{a}\lambda_1+\bar{b}\lambda_2-g^*\lambda_3)\|e(t)\|^2\\&=-\|e(t)\|^2\\&=-2M(t),\end{aligned}\tag{9}$$

where $\lambda_3 = \lambda_{\min}(I_{\mathfrak{M}\mathfrak{N}} \otimes (\Gamma^T\Gamma))$ and $M(t) = \frac{1}{2}\sum_{\kappa=1}^{\mathfrak{M}}\sum_{\imath=1}^{\mathfrak{N}}(e_\imath^{(\kappa)}(t))^T e_\imath^{(\kappa)}(t)$. By means of Lemma 1, one obtains

$$M(t) \leqslant V(t) + 2{}_{t_0}^{C}I_t^{\bar{\alpha}}M(t) \leqslant V(t_0),$$

which implies that $M(t)$ and ${}_{t_0}^{C}I_t^{\bar{\alpha}}M(t)$ are bounded for $t \geqslant t_0$. Furthermore,

$$\lim_{t\to+\infty} M(t) = 0,$$

which is derived by the proof of Theorem 2 in [28]. From the definition of $M(t)$, $\lim_{t\to+\infty}\|e_\imath^{(\kappa)}(t)\| = 0$. Thus, System (1) is asymptotically synchronized. □

Remark 1. *When $\bar{b} = 0$, System (1) is reduced to*

$$\begin{cases} {}_{t_0}^{C}D_t^{\bar{\alpha}}x_\imath^{(\kappa)}(t) = \bar{f}(x_\imath^{(\kappa)}(t)) + \bar{a}\sum\limits_{\jmath=1}^{\mathfrak{N}} l_{\imath\jmath}^{(\kappa)}Hz_\jmath^{(\kappa)}(t) + u_\imath^{(\kappa)}(t), \\ z_\imath^{(\kappa)}(t) = \Gamma x_\imath^{(\kappa)}(t), \quad \imath \in \tilde{\mathfrak{N}}, \kappa \in \tilde{\mathfrak{M}}. \end{cases} \tag{10}$$

From the analysis of Theorem 1, it is easy to conclude that the FOOCMN without inter-layer coupling (10) is also asymptotically synchronized under Assumption 1 and Controller (4).

Remark 2. *Similarly, $\bar{a} = 0$, System (1) is reduced as*

$$\begin{cases} {}_{t_0}^{C}D_t^{\bar{\alpha}}x_\imath^{(\kappa)}(t) = \bar{f}(x_\imath^{(\kappa)}(t)) + \bar{b}\sum\limits_{\bar{\imath}=1}^{\mathfrak{M}} d_{\kappa\bar{\imath}}Pz_\imath^{(\bar{\imath})}(t) + u_\imath^{(\kappa)}(t), \\ z_\imath^{(\kappa)}(t) = \Gamma x_\imath^{(\kappa)}(t), \quad \imath \in \tilde{\mathfrak{N}}, \kappa \in \tilde{\mathfrak{M}}. \end{cases} \tag{11}$$

Under Assumption 1 and Controller (4), the FOOCMN without intra-layer coupling (11) can achieve asymptotic synchronization.

Remark 3. *At present, the models of the multiplex network in most articles are two-layer networks, such as in [40–42]. In contrast, the model in this paper can contain multiple layers, which is more complex and realistic.*

If $\bar{\alpha} = 1$, System (1) becomes the following integer-order network:

$$\begin{cases} \dot{x}_\imath^{(\kappa)}(t) = \bar{f}(x_\imath^{(\kappa)}(t)) - \bar{a}\sum\limits_{\jmath=1}^{\mathfrak{N}} l_{\imath\jmath}^{(\kappa)}Hz_\jmath^{(\kappa)}(t) - \bar{b}\sum\limits_{\bar{\imath}=1}^{\mathfrak{M}} d_{\kappa\bar{\imath}}Pz_\imath^{(\bar{\imath})}(t) + u_\imath^{(\kappa)}(t), \\ z_\imath^{(\kappa)}(t) = \Gamma x_\imath^{(\kappa)}(t), \qquad \imath \in \tilde{\mathfrak{N}}, \kappa \in \tilde{\mathfrak{M}}. \end{cases} \tag{12}$$

In light of this, Adaptive Controller (4) assumes the following form:

$$\begin{cases} u_\imath^{(\kappa)}(t) = -g_\imath^{(\kappa)}(t)\Gamma^T\theta_\imath^{(\kappa)}(t), \\ \dot{g}_\imath^{(\kappa)}(t) = \beta_\imath^{(\kappa)}\left\|\theta_\imath^{(\kappa)}(t)\right\|^2, \quad \imath \in \tilde{\mathfrak{N}}, \kappa \in \tilde{\mathfrak{M}}. \end{cases} \tag{13}$$

Corollary 1. *Under Assumption 1, Network (12) achieves asymptotic synchronization via Adaptive Controller (13).*

Proof. Constructing the same Lyapunov function as in Theorem 1, one has

$$\begin{aligned}\dot{V}(t) \leq& \sum_{\kappa=1}^{\mathfrak{M}} \sum_{\imath=1}^{\mathfrak{N}} (e_\imath^{(\kappa)}(t))^T \dot{e}_\imath^{(\kappa)}(t) + \sum_{\kappa=1}^{\mathfrak{M}} \sum_{\imath=1}^{\mathfrak{N}} \frac{1}{\beta_\imath^{(\kappa)}} (g_\imath^{(\kappa)}(t) - g^*) \dot{g}_\imath^{(\kappa)}(t) \\ =& \sum_{\kappa=1}^{\mathfrak{M}} \sum_{\imath=1}^{\mathfrak{N}} (e_\imath^{(\kappa)}(t))^T \Big[\tilde{f}(e_\imath^{(\kappa)}(t)) - \bar{a} \sum_{\jmath=1}^{\mathfrak{N}} l_{\imath\jmath}^{(\kappa)} H \theta_\jmath^{(\kappa)}(t) \\ &- \bar{b} \sum_{\bar{\imath}=1}^{\mathfrak{M}} d_{\kappa\bar{\imath}} P \theta_\imath^{(\bar{\imath})}(t) + u_\imath^{(\kappa)}(t) \Big] + \sum_{\kappa=1}^{\mathfrak{M}} \sum_{\imath=1}^{\mathfrak{N}} (g_\imath^{(\kappa)}(t) - g^*) \left\| \theta_\imath^{(\kappa)}(t) \right\|^2 \\ =& \sum_{\kappa=1}^{\mathfrak{M}} \sum_{\imath=1}^{\mathfrak{N}} (e_\imath^{(\kappa)}(t))^T \tilde{f}(e_\imath^{(\kappa)}(t)) - \bar{a} \sum_{\kappa=1}^{\mathfrak{M}} \sum_{\imath=1}^{\mathfrak{N}} \sum_{\jmath=1}^{\mathfrak{N}} (e_\imath^{(\kappa)}(t))^T l_{\imath\jmath}^{(\kappa)} H \theta_\jmath^{(\kappa)}(t) \\ &- \bar{b} \sum_{\kappa=1}^{\mathfrak{M}} \sum_{\imath=1}^{\mathfrak{N}} \sum_{\bar{\imath}=1}^{\mathfrak{M}} (e_\imath^{(\kappa)}(t))^T d_{\kappa\bar{\imath}} P \theta_\imath^{(\bar{\imath})}(t) - \sum_{\kappa=1}^{\mathfrak{M}} \sum_{\imath=1}^{\mathfrak{N}} g^* \left\| \theta_\imath^{(\kappa)}(t) \right\|^2 \\ \leq& (\ell_f + \bar{a}\lambda_1 + \bar{b}\lambda_2 - g^*\lambda_3) \|e(t)\|^2. \end{aligned}$$

We choose $g^* \geq \frac{\ell_f + \bar{a}\lambda_1 + \bar{b}\lambda_2 + 1}{\lambda_3}$, which leads to $\dot{V}(t) \leq 0$. Thus, System (12) is asymptotically synchronized. □

If $m = n$ and $\Gamma = I$, System (1) becomes the following fractional-order multiplex network:

$$\begin{aligned} {}_{t_0}^{C}D_t^{\bar{\alpha}} x_\imath^{(\kappa)}(t) =& \bar{f}\left(x_\imath^{(\kappa)}(t)\right) - \bar{a} \sum_{\jmath=1}^{\mathfrak{N}} l_{\imath\jmath}^{(\kappa)} H x_\jmath^{(\kappa)}(t) \\ &- \bar{b} \sum_{\bar{\imath}=1}^{\mathfrak{M}} d_{\kappa\bar{\imath}} P x_\imath^{(\bar{\imath})}(t) + u_\imath^{(\kappa)}(t), \quad \imath \in \tilde{\mathfrak{N}}, \kappa \in \tilde{\mathfrak{M}}. \end{aligned} \tag{14}$$

The error system is described as

$$\begin{aligned} {}_{t_0}^{C}D_t^{\bar{\alpha}} e_\imath^{(\kappa)}(t) =& \tilde{f}(e_\imath^{(\kappa)}(t)) - \bar{a} \sum_{\jmath=1}^{\mathfrak{N}} l_{\imath\jmath}^{(\kappa)} H e_\jmath^{(\kappa)}(t) \\ &- \bar{b} \sum_{\bar{\imath}=1}^{\mathfrak{M}} d_{\kappa\bar{\imath}} P e_\imath^{(\bar{\imath})}(t) + \hat{u}_\imath^{(\kappa)}(t), \quad \imath \in \tilde{\mathfrak{N}}, \kappa \in \tilde{\mathfrak{M}}. \end{aligned} \tag{15}$$

Accordingly, the adaptive controller is designed as

$$\begin{cases} \hat{u}_\imath^{(\kappa)}(t) = -\hat{g}_\imath^{(\kappa)}(t) e_\imath^{(\kappa)}(t), \\ {}_{t_0}^{C}D_t^{\bar{\alpha}} \hat{g}_\imath^{(\kappa)}(t) = \hat{\beta}_\imath^{(\kappa)} \left\| e_\imath^{(\kappa)}(t) \right\|^2, \quad \imath \in \tilde{\mathfrak{N}}, \kappa \in \tilde{\mathfrak{M}}. \end{cases} \tag{16}$$

Corollary 2. *Under Assumption 1 and Adaptive Law (16), Network (14) achieves asymptotic synchronization.*

Proof. Construct a Lyapunov function

$$V(t) = \frac{1}{2} \sum_{\kappa=1}^{\mathfrak{M}} \sum_{\imath=1}^{\mathfrak{N}} (e_\imath^{(\kappa)}(t))^T e_\imath^{(\kappa)}(t) + \frac{1}{2} \sum_{\kappa=1}^{\mathfrak{M}} \sum_{\imath=1}^{\mathfrak{N}} \frac{1}{\hat{\beta}_\imath^{(\kappa)}} \left(\hat{g}_\imath^{(\kappa)}(t) - \hat{g}^* \right)^2,$$

where $\hat{g}^*$ is an adaptive constant.

Similar to the proof of Theorem 1, one has

$$\begin{aligned}
{}_{t_0}^{C}D_t^{\bar{\alpha}}V(t) \leq& \sum_{\kappa=1}^{\mathfrak{M}}\sum_{\imath=1}^{\mathfrak{N}}(e_\imath^{(\kappa)}(t))^T {}_{t_0}^{C}D_t^{\bar{\alpha}}e_\imath^{(\kappa)}(t) + \sum_{\kappa=1}^{\mathfrak{M}}\sum_{\imath=1}^{\mathfrak{N}}\frac{1}{\hat{\beta}_\imath^{(\kappa)}}\left(\hat{g}_\imath^{(\kappa)}(t)-\hat{g}^*\right){}_{t_0}^{C}D_t^{\bar{\alpha}}\hat{g}_\imath^{(\kappa)}(t)\\
=& \sum_{\kappa=1}^{\mathfrak{M}}\sum_{\imath=1}^{\mathfrak{N}}(e_\imath^{(\kappa)}(t))^T\Big[\tilde{f}(e_\imath^{(\kappa)}(t)) - \bar{a}\sum_{\jmath=1}^{\mathfrak{N}}l_{\imath\jmath}^{(\kappa)}He_\jmath^{(\kappa)}(t)\\
&-\bar{b}\sum_{\bar{\imath}=1}^{\mathfrak{M}}d_{\kappa\bar{\imath}}Pe_\imath^{(\bar{\imath})}(t)+u_\imath^{(\kappa)}(t)\Big] + \sum_{\kappa=1}^{\mathfrak{M}}\sum_{\imath=1}^{\mathfrak{N}}\left(\hat{g}_\imath^{(\kappa)}(t)-\hat{g}^*\right)\left\|e_\imath^{(\kappa)}(t)\right\|^2\\
=& \sum_{\kappa=1}^{\mathfrak{M}}\sum_{\imath=1}^{\mathfrak{N}}(e_\imath^{(\kappa)}(t))^T\tilde{f}(e_\imath^{(\kappa)}(t)) - \bar{a}\sum_{\kappa=1}^{\mathfrak{M}}\sum_{\imath=1}^{\mathfrak{N}}\sum_{\jmath=1}^{\mathfrak{N}}(e_\imath^{(\kappa)}(t))^T l_{\imath\jmath}^{(k)}He_\jmath^{(\kappa)}(t)\\
&-\bar{b}\sum_{\kappa=1}^{\mathfrak{M}}\sum_{\imath=1}^{\mathfrak{N}}\sum_{\bar{\imath}=1}^{\mathfrak{M}}(e_\imath^{(\kappa)}(t))^T d_{\kappa\bar{\imath}}Pe_\imath^{(\bar{\imath})}(t) - \sum_{\kappa=1}^{\mathfrak{M}}\sum_{\imath=1}^{\mathfrak{N}}\hat{g}^*(e_\imath^{(\kappa)}(t))^T e_\imath^{(\kappa)}(t)\\
\leq& (\ell_f+\bar{a}\lambda_1+\bar{b}\lambda_2-\hat{g}^*)\|e(t)\|^2.
\end{aligned}$$

We choose $\hat{g}^* = \ell_f + \bar{a}\lambda_1 + \bar{b}\lambda_2 + 1$, which leads to ${}_{t_0}^{C}D_t^{\bar{\alpha}}V(t) \leq -\|e(t)\|^2$. The rest of the proof is similar to that of Theorem 1. □

Remark 4. *Obviously, Network (14) is a special case of Network (1), and the coupling term is state coupling. The coupling term in the fractional multiplex network models studied in [29,30] are also state coupling, but Network (1) has the item of output coupling, which is more general.*

3.2. Adaptive Quantized Synchronization

The process of quantization can be thought as the process of coding, which maps a continuous signal to a piecewise constant signal.

The adaptive quantized control protocol here $\bar{u}_\imath^{(\kappa)}(t)$ is developed as

$$\begin{cases} \bar{u}_\imath^{(\kappa)}(t) = -\bar{g}_\imath^{(\kappa)}(t)\Gamma^T q(\theta_\imath^{(\kappa)}(t)),\\ {}_{t_0}^{C}D_t^{\bar{\alpha}}\bar{g}_\imath^{(\kappa)}(t) = \bar{\beta}_\imath^{(\kappa)}\|\theta_\imath(t)\|^2, \quad \imath\in\tilde{\mathfrak{N}},\kappa\in\tilde{\mathfrak{M}}, \end{cases} \tag{17}$$

where $\bar{\beta}_\imath^{(\kappa)} > 0$, $\bar{g}_\imath^{(\kappa)}(t) > 0$, $q(\theta_\imath^{(\kappa)}(t)) = \left(\tilde{q}(\theta_{\imath_1}^{(\kappa)}(t)), \tilde{q}(\theta_{\imath_2}^{(\kappa)}(t)), \ldots, \tilde{q}(\theta_{\imath_m}^{(\kappa)}(t))\right)^T$.

The quantizer $\tilde{q}(\cdot) : \mathbb{R} \to \mathcal{V}$ is defined as follows:

$$\tilde{q}(\tau) = \begin{cases} \xi_\varsigma, & \frac{1}{1+\delta}\xi_\varsigma < \tau \leq \frac{1}{1-\delta}\xi_\varsigma,\\ 0, & \tau = 0,\\ -\tilde{q}(-\tau), & \tau < 0, \end{cases}$$

where $\mathcal{V} = \{\pm\xi_\varsigma : \xi_\varsigma = \rho^\varsigma\xi_0, \varsigma = 0, \pm1, \pm2, \ldots\} \cup \{0\}$ with $\xi_0 > 0$, and $\delta = \frac{1-\rho}{1+\rho}$, $0 < \rho < 1$. In the sense of Filippov, there exists $\Delta \in [-\delta, \delta]$ such that $\tilde{q}(\tau) = (1+\Delta)\tau$, $\tau \in \mathbb{R}$.

Theorem 2. *Based on Assumption 1, FOOCMN (1) achieves synchronization under Adaptive Quantized Controller (17).*

Proof. Construct a Lyapunov function as follows:

$$\bar{V}(t) = \frac{1}{2}\sum_{\kappa=1}^{\mathfrak{M}}\sum_{\imath=1}^{\mathfrak{N}}(e_\imath^{(\kappa)}(t))^T e_\imath^{(\kappa)}(t) + \frac{1}{2}\sum_{\kappa=1}^{\mathfrak{M}}\sum_{\imath=1}^{\mathfrak{N}}\frac{1-\delta}{\bar{\beta}_\imath^{(\kappa)}}\left(\bar{g}_\imath^{(\kappa)}(t) - \bar{g^*}\right)^2,$$

where $\bar{g^*}$ is an adaptive number.

Similarly to Theorem 1, one obtains that

$$
\begin{aligned}
{}_{t_0}^{C}D_t^{\bar{\alpha}}\bar{V}(t) \leq& \sum_{\kappa=1}^{\mathfrak{M}}\sum_{\imath=1}^{\mathfrak{N}}(e_\imath^{(\kappa)}(t))^T {}_{t_0}^{C}D_t^{\bar{\alpha}} e_\imath^{(\kappa)}(t) + \sum_{\kappa=1}^{\mathfrak{M}}\sum_{\imath=1}^{\mathfrak{N}} \frac{1-\delta}{\bar{\beta}_\imath^{(\kappa)}}\left(\bar{g}_\imath^{(\kappa)}(t)-\bar{g^*}\right){}_{t_0}^{C}D_t^{\bar{\alpha}}\bar{g}_\imath^{(\kappa)}(t) \\
=& \sum_{\kappa=1}^{\mathfrak{M}}\sum_{\imath=1}^{\mathfrak{N}}(e_\imath^{(\kappa)}(t))^T\Big[\bar{f}(x_\imath^{(\kappa)}(t)) - \bar{f}(s(t)) - \bar{a}\sum_{\jmath=1}^{N} l_{\imath\jmath}^{(\kappa)} H\theta_\jmath^{(\kappa)}(t) \\
&- \bar{b}\sum_{\bar{\imath}=1}^{\mathfrak{M}} d_{\kappa\bar{\imath}}P\theta_\imath^{(\bar{\imath})}(t) + \bar{u}_\imath^{(\kappa)}(t)\Big] \\
&+ (1-\delta)\sum_{\kappa=1}^{\mathfrak{M}}\sum_{\imath=1}^{\mathfrak{N}}\left(\bar{g}_\imath^{(\kappa)}(t)-\bar{g^*}\right)\|e_\imath^{(\kappa)}(t)\|^2 \\
=& \sum_{\kappa=1}^{\mathfrak{M}}\sum_{\imath=1}^{\mathfrak{N}}(e_\imath^{(\kappa)}(t))^T\tilde{f}(e_\imath^{(\kappa)}(t)) - \bar{a}\sum_{\kappa=1}^{\mathfrak{M}}\sum_{\imath=1}^{\mathfrak{N}}\sum_{\jmath=1}^{\mathfrak{N}}(e_\imath^{(\kappa)}(t))^T l_{\imath\jmath}^{(\kappa)} He_\jmath^{(\kappa)}(t) \\
&- \bar{b}\sum_{\kappa=1}^{\mathfrak{M}}\sum_{\imath=1}^{\mathfrak{N}}\sum_{\bar{\imath}=1}^{\mathfrak{M}}(e_\imath^{(\kappa)}(t))^T d_{\kappa\bar{\imath}}Pe_\imath^{(\bar{\imath})}(t) - \sum_{\kappa=1}^{\mathfrak{M}}\sum_{\imath=1}^{\mathfrak{N}}\bar{g}_\imath^{(\kappa)}(t)(e_\imath^{(\kappa)}(t))^T\Gamma^T q(\theta_\imath^{(\kappa)}(t)) \\
&+ (1-\delta)\sum_{\kappa=1}^{\mathfrak{M}}\sum_{\imath=1}^{\mathfrak{N}}\left(\bar{g}_\imath^{(\kappa)}(t)-\bar{g^*}\right)\|\theta_\imath^{(\kappa)}(t)\|^2.
\end{aligned}
$$

By the property of quantization, we have

$$
\begin{aligned}
&- \sum_{\kappa=1}^{\mathfrak{M}}\sum_{\imath=1}^{\mathfrak{N}}\bar{g}_\imath^{(\kappa)}(t)(e_\imath^{(\kappa)}(t))^T\Gamma^T q(\theta_\imath^{(\kappa)}(t)) \\
=& - \sum_{\kappa=1}^{\mathfrak{M}}\sum_{\imath=1}^{\mathfrak{N}}\bar{g}_\imath^{(\kappa)}(t)(\theta_\imath^{(\kappa)}(t))^T q(\theta_\imath^{(\kappa)}(t)) \\
=& - \sum_{\kappa=1}^{\mathfrak{M}}\sum_{\imath=1}^{\mathfrak{N}}\sum_{\bar{\varrho}=1}^{m}\bar{g}_\imath^{(\kappa)}(t)(\theta_{\imath\bar{\varrho}}^{(\kappa)}(t))^T \tilde{q}(\theta_{\imath\bar{\varrho}}^{(\kappa)}(t)).
\end{aligned} \tag{18}
$$

When $\theta_{\imath\bar{\varrho}}^{(\kappa)}(t) \geq 0$,

$$
\begin{aligned}
&\sum_{\kappa=1}^{\mathfrak{M}}\sum_{\imath=1}^{\mathfrak{N}}\sum_{\bar{\varrho}=1}^{m}\bar{g}_\imath^{(\kappa)}(t)(\theta_{\imath\bar{\varrho}}^{(\kappa)}(t))^T \tilde{q}(\theta_{\imath\bar{\varrho}}^{(\kappa)}(t)) \\
\geq& (1-\delta)\sum_{\kappa=1}^{\mathfrak{M}}\sum_{\imath=1}^{\mathfrak{N}}\sum_{\bar{\varrho}=1}^{m}\bar{g}_\imath^{(\kappa)}(t)(\theta_{\imath\bar{\varrho}}^{(\kappa)}(t))^T \theta_{\imath\bar{\varrho}}^{(\kappa)}(t),
\end{aligned} \tag{19}
$$

When $\theta_{\imath\bar{\varrho}}^{(\kappa)}(t) < 0$,

$$
\begin{aligned}
&\sum_{\kappa=1}^{\mathfrak{M}}\sum_{\imath=1}^{\mathfrak{N}}\sum_{\bar{\varrho}=1}^{m}\bar{g}_\imath^{(\kappa)}(t)(\theta_{\imath\bar{\varrho}}^{(\kappa)}(t))^T \tilde{q}(\theta_{\imath\bar{\varrho}}^{(\kappa)}(t)) \\
=& - \sum_{\kappa=1}^{\mathfrak{M}}\sum_{\imath=1}^{\mathfrak{N}}\sum_{\bar{\varrho}=1}^{m}\bar{g}_\imath^{(\kappa)}(t)(\theta_{\imath\bar{\varrho}}^{(\kappa)}(t))^T \tilde{q}(-\theta_{\imath\bar{\varrho}}^{(\kappa)}(t)) \\
>& (1-\delta)\sum_{\kappa=1}^{\mathfrak{M}}\sum_{\imath=1}^{\mathfrak{N}}\sum_{\bar{\varrho}=1}^{m}\bar{g}_\imath^{(\kappa)}(t)(-\theta_{\imath\bar{\varrho}}^{(\kappa)}(t))^T (-\theta_{\imath\bar{\varrho}}^{(\kappa)}(t)) \\
=& (1-\delta)\sum_{\kappa=1}^{\mathfrak{M}}\sum_{\imath=1}^{\mathfrak{N}}\sum_{\bar{\varrho}=1}^{m}\bar{g}_\imath^{(\kappa)}(t)(\theta_{\imath\bar{\varrho}}^{(\kappa)}(t))^T \theta_{\imath\bar{\varrho}}^{(\kappa)}(t).
\end{aligned} \tag{20}
$$

From (19)–(20), it follows that

$$
\begin{aligned}
&-\sum_{\kappa=1}^{\mathfrak{M}}\sum_{\imath=1}^{\mathfrak{N}}\bar{g}_\imath^{(\kappa)}(t)(\theta_\imath^{(\kappa)}(t))^T q(\theta_\imath^{(\kappa)}(t))\\
\leq&-(1-\delta)\sum_{\kappa=1}^{\mathfrak{M}}\sum_{\imath=1}^{\mathfrak{N}}\bar{g}_\imath^{(\kappa)}(t)(\theta_\imath^{(\kappa)}(t))^T\theta_\imath^{(\kappa)}(t).
\end{aligned}
$$

From the above analysis, one has

$$
\begin{aligned}
{}_{t_0}^{C}D_t^{\alpha}\bar{V}(t) \leq&(\ell_f+\bar{a}\lambda_1+\bar{b}\lambda_2)\|e(t)\|^2\\
&-(1-\delta)\sum_{\kappa=1}^{\mathfrak{M}}\sum_{\imath=1}^{\mathfrak{N}}\bar{g}_\imath^{(\kappa)}(t)(\theta_\imath^{(\kappa)}(t))^T\theta_\imath^{(\kappa)}(t)\\
&+(1-\delta)\sum_{\kappa=1}^{\mathfrak{M}}\sum_{\imath=1}^{\mathfrak{N}}\left(\bar{g}_\imath^{(\kappa)}(t)-\bar{g^*}\right)\|\theta_\imath^{(\kappa)}(t)\|^2\\
=&(\ell_f+\bar{a}\lambda_1+\bar{b}\lambda_2)\|e(t)\|^2-(1-\delta)\bar{g}^*e^T(t)(I_{\mathfrak{M}\mathfrak{N}}\otimes(\Gamma^T\Gamma))e(t)\\
\leq&(\ell_f+\bar{a}\lambda_1+\bar{b}\lambda_2-(1-\delta)\bar{g^*}\lambda_3)\|e(t)\|^2.
\end{aligned}
$$

Choosing $\bar{g^*}=\frac{\ell_f+\bar{a}\lambda_1+\bar{b}\lambda_2+1}{(1-\delta)\lambda_3}$, we can also obtain ${}_{t_0}^{C}D_t^{\alpha}\bar{V}(t)\leq -e^T(t)e(t)$. Therefore, FOOCMN (1) is asymptotically synchronized. □

Remark 5. *Under Assumption 1 and Controller (17), the FOOCMN without inter-layer coupling (10) or without intra-layer coupling (11) can also achieve synchronization. Note that Systems (10) and (11) are special cases of multiplex networks, which has been studied in [43,44]. Therefore, the FOOCMNs studied in this article are more general.*

If $\bar{\alpha}=1$, Adaptive Quantized Controller (17) assumes the following form:

$$
\begin{cases}
\bar{u}_\imath^{(\kappa)}(t)=-\bar{g}_\imath^{(\kappa)}(t)\Gamma^T q(\theta_\imath^{(\kappa)}(t)),\\
\dot{\bar{g}}_\imath^{(\kappa)}(t)=\bar{\beta}_\imath^{(\kappa)}\|\theta_\imath(t)\|^2, \qquad \imath\in\mathfrak{N},\kappa\in\mathfrak{M}.
\end{cases}
\tag{21}
$$

Corollary 3. *Under Assumption 1, the integer-order network (12) achieves asymptotic synchronization via the adaptive quantized control (21).*

Proof. Constructing the same Lyapunov function as Theorem 2, one has

$$
\begin{aligned}
\dot{V}(t)\leq&\sum_{\kappa=1}^{\mathfrak{M}}\sum_{\imath=1}^{\mathfrak{N}}(e_\imath^{(\kappa)}(t))^T\dot{e}_\imath^{(\kappa)}(t)+\sum_{\kappa=1}^{\mathfrak{M}}\sum_{\imath=1}^{\mathfrak{N}}\frac{1-\delta}{\bar{\beta}_\imath^{(\kappa)}}\left(\bar{g}_\imath^{(\kappa)}(t)-\bar{g^*}\right)\dot{\bar{g}}_\imath^{(\kappa)}(t)\\
=&\sum_{\kappa=1}^{\mathfrak{M}}\sum_{\imath=1}^{\mathfrak{N}}(e_\imath^{(\kappa)}(t))^T\tilde{f}(e_\imath^{(\kappa)}(t))-\bar{a}\sum_{\kappa=1}^{\mathfrak{M}}\sum_{\imath=1}^{\mathfrak{N}}\sum_{\jmath=1}^{\mathfrak{N}}(e_\imath^{(\kappa)}(t))^T l_{\imath\jmath}^{(\kappa)}He_\jmath^{(\kappa)}(t)\\
&-\bar{b}\sum_{\kappa=1}^{\mathfrak{M}}\sum_{\imath=1}^{\mathfrak{N}}\sum_{\bar{\imath}=1}^{\mathfrak{M}}(e_\imath^{(\kappa)}(t))^T d_{\kappa\bar{\imath}}Pe_\imath^{(\bar{\imath})}(t)-\sum_{\kappa=1}^{\mathfrak{M}}\sum_{\imath=1}^{\mathfrak{N}}\bar{g}_\imath^{(\kappa)}(t)(e_\imath^{(\kappa)}(t))^T\Gamma^T q(\theta_\imath^{(\kappa)}(t))\\
&+(1-\delta)\sum_{\kappa=1}^{\mathfrak{M}}\sum_{\imath=1}^{\mathfrak{N}}\left(\bar{g}_\imath^{(\kappa)}(t)-\bar{g^*}\right)\|\theta_\imath^{(\kappa)}(t)\|^2\\
\leq&(\ell_f+\bar{a}\lambda_1+\bar{b}\lambda_2-(1-\delta)\bar{g^*}\lambda_3)\|e(t)\|^2.
\end{aligned}
$$

We choose $\bar{g^*}\geq\frac{\ell_f+\bar{a}\lambda_1+\bar{b}\lambda_2+1}{(1-\delta)\lambda_3}$, which leads to $\dot{V}(t)\leq -\|e(t)\|^2$, and System (12) is asymptotically synchronized. □

Remark 6. *Compared with the results in [45,46], where the dynamic behaviors are described by the integer-order systems, the systems in this article are fractional-order models. According to Corollary 1 and Corollary 3, the results of this paper are also applicable for the integer-order multiplex networks, so it can be considered a valuable extension from integer-order multiplex networks to fractional-order ones.*

If $m = n$ and $\Gamma = I$, Controller (17) assumes the following form:

$$\begin{cases} \bar{u}_\imath^{(\kappa)}(t) = -\bar{g}_\imath^{(\kappa)}(t)q(e_\imath^{(\kappa)}(t)), \\ {}_0^C D_t^{\bar{\alpha}} \bar{g}_\imath^{(\kappa)}(t) = \bar{\beta}_\imath^{(\kappa)} \|e_\imath(t)\|^2, \qquad \imath \in \tilde{\mathfrak{N}}, \kappa \in \tilde{\mathfrak{M}}. \end{cases} \tag{22}$$

Corollary 4. *Based on Assumption 1 and Controller (22), FOOCMN (14) achieves asymptotic synchronization.*

Proof. We construct a Lyapunov function of the following form:

$$\bar{V}(t) = \frac{1}{2}\sum_{\kappa=1}^{\mathfrak{M}}\sum_{\imath=1}^{\mathfrak{N}}(e_\imath^{(\kappa)}(t))^T e_\imath^{(\kappa)}(t) + \frac{1}{2}\sum_{\kappa=1}^{\mathfrak{M}}\sum_{\imath=1}^{\mathfrak{N}}\frac{1-\delta}{\bar{\beta}_\imath^{(\kappa)}}(\bar{g}_\imath^{(\kappa)}(t) - \bar{g}^*)^2.$$

Similar to Theorem 2, choosing $\bar{g}^* = \frac{1}{1-\delta}(\ell_f + \bar{a}\lambda_1 + \bar{b}\lambda_2 + 1)$, one obtains that

$$\begin{aligned} {}_0^C D_t^{\bar{\alpha}} \bar{V}(t) \leq & \sum_{\kappa=1}^{\mathfrak{M}}\sum_{\imath=1}^{\mathfrak{N}}(e_\imath^{(\kappa)}(t))^T {}_0^C D_t^{\bar{\alpha}} e_\imath^{(\kappa)}(t) + \sum_{\kappa=1}^{\mathfrak{M}}\sum_{\imath=1}^{\mathfrak{N}}\frac{1-\delta}{\bar{\beta}_\imath^{(\kappa)}}(\bar{g}_\imath^{(\kappa)}(t) - \bar{g}^*){}_0^C D_t^{\bar{\alpha}} \bar{g}_\imath^{(\kappa)}(t) \\ = & \sum_{\kappa=1}^{\mathfrak{M}}\sum_{\imath=1}^{\mathfrak{N}}(e_\imath^{(\kappa)}(t))^T \tilde{f}(e_\imath^{(\kappa)}(t)) - \bar{a}\sum_{\kappa=1}^{\mathfrak{M}}\sum_{\imath=1}^{\mathfrak{N}}\sum_{\jmath=1}^{\mathfrak{N}} l_{\imath\jmath}^{(\kappa)}(e_\imath^{(\kappa)}(t))^T H e_\jmath^{(\kappa)}(t) \\ & - \bar{b}\sum_{\kappa=1}^{\mathfrak{M}}\sum_{\imath=1}^{\mathfrak{N}}\sum_{\bar{\imath}=1}^{\mathfrak{M}} d_{\kappa\bar{\imath}}(e_\imath^{(\kappa)}(t))^T P e_\imath^{(\bar{\imath})}(t) - \sum_{\kappa=1}^{\mathfrak{M}}\sum_{\imath=1}^{\mathfrak{N}}\bar{g}_\imath^{(\kappa)}(t)(e_\imath^{(\kappa)}(t))^T q(e_\imath^{(\kappa)}(t)) \\ & + (1-\delta)\sum_{\kappa=1}^{\mathfrak{M}}\sum_{\imath=1}^{\mathfrak{N}}(\bar{g}_\imath^{(\kappa)}(t) - \bar{g}^*)\|e_\imath^{(\kappa)}(t)\|^2 \\ \leq & (\ell_f + \bar{a}\lambda_1 + \bar{b}\lambda_2 - (1-\delta)\bar{g}^*)\|e(t)\|^2 \\ = & -\|e(t)\|^2. \end{aligned}$$

The rest of the proof is similar to that of Theorem 2. □

Remark 7. *In fact, quantization is a process of discretizing continuous signals, which can effectively reduce the load on the communication channel during signal transmission. Although there are some research achievements on quantitative control [32,33], there are few studies on the quantitative control of FOOCMNs. In this paper, the synchronization problem of FOOCMNs is studied by introducing adaptive quantitative control.*

4. Numerical Example

Two numerical examples are shown in this section to support the theoretical analysis.

Consider a FOOCMN consisting of 3 layers, in which each layer consists of 3 nodes, whose topology is depicted in Figure 1. Selecting the chaotic L*ü*'s system, Lorenz system, and Rössler system as the synchronization state of each layer, they can be described as

$${}_0^C D_t^{\bar{\alpha}} s^{(1)}(t) = \begin{pmatrix} f_1^{(1)}(s(t)) \\ f_2^{(1)}(s(t)) \\ f_3^{(1)}(s(t)) \end{pmatrix} = \begin{pmatrix} 12s_2^{(1)}(t) - 10s_1^{(1)}(t) \\ 20s_1^{(1)}(t) - 2.5s_1^{(1)}(t)s_3^{(1)}(t) \\ 4s_1^{(1)}(t)s_1^{(1)}(t) - 3s_3^{(1)}(t) \end{pmatrix}, \tag{23}$$

$$
{}_{0}^{C}D_{t}^{\bar{\alpha}}s^{(2)}(t)=\begin{pmatrix} f_1^{(2)}(s(t)) \\ f_2^{(2)}(s(t)) \\ f_3^{(2)}(s(t)) \end{pmatrix}=\begin{pmatrix} 10(s_2^{(2)}(t)-s_1^{(2)}(t)) \\ 28s_1^{(2)}(t)-s_2^{(2)}(t)-s_1^{(2)}(t)s_3^{(2)}(t) \\ s_2^{(2)}(t)s_1^{(2)}(t)-\frac{8}{3}s_3^{(2)}(t) \end{pmatrix}, \tag{24}
$$

$$
{}_{0}^{C}D_{t}^{\bar{\alpha}}s^{(3)}(t)=\begin{pmatrix} f_1^{(3)}(s(t)) \\ f_2^{(3)}(s(t)) \\ f_3^{(3)}(s(t)) \end{pmatrix}=\begin{pmatrix} -(s_2^{(3)}(t)+s_3^{(3)}(t)) \\ s_1^{(3)}(t)+0.2s_2^{(3)}(t) \\ s_1^{(3)}(t)s_3^{(3)}(t)-18s_3^{(3)}(t)+0.2 \end{pmatrix}. \tag{25}
$$

Choosing $\bar{\alpha}=0.98$, the dynamical behavior of Systems (23)−(25) are simulated in Figures 2–4 with initial values $s(0)=(1,2.5,6)^T$.

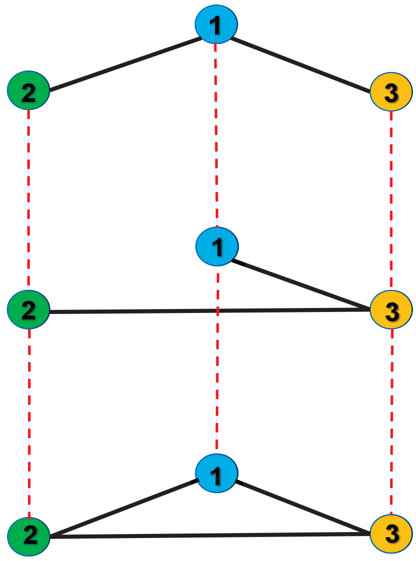

Figure 1. Topology of the multiplex network (1).

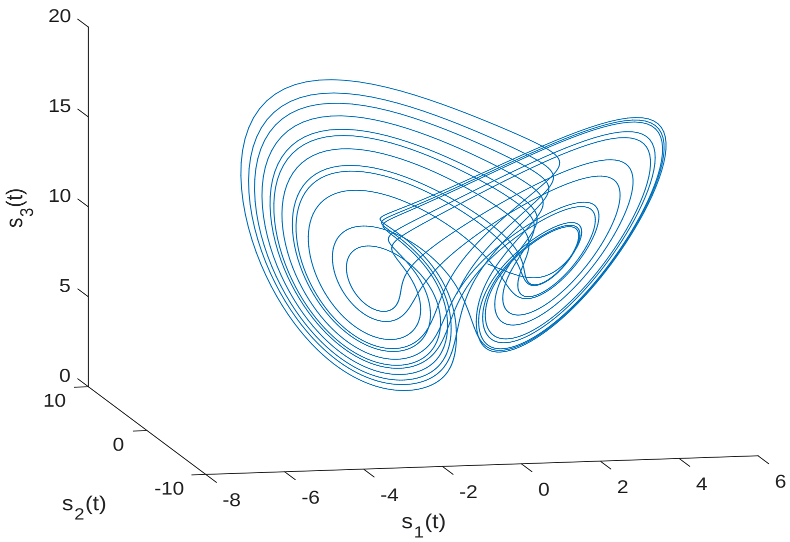

Figure 2. The chaotic behavior of System (23).

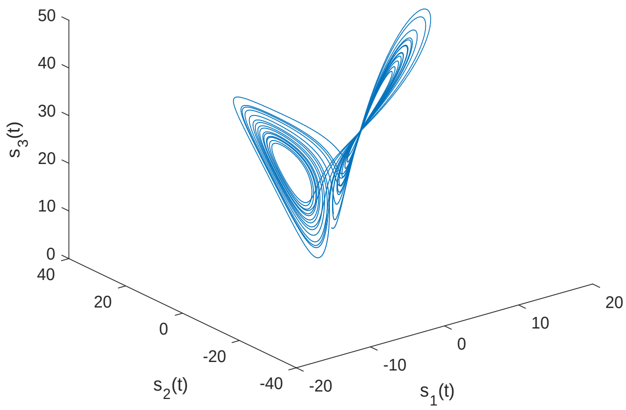

Figure 3. The chaotic behavior of System (24).

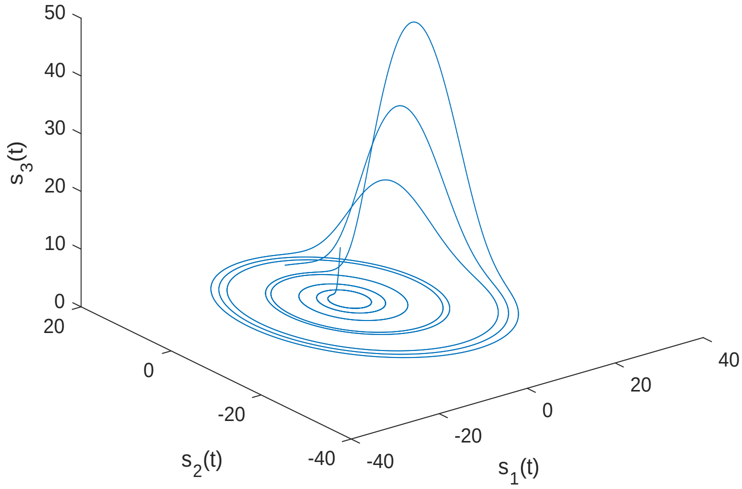

Figure 4. The chaotic behavior of System (25).

Example 1. *Consider FOOCMN (1), where* $\mathfrak{N} = \mathfrak{M} = 3$, $x_\imath^{(\kappa)} = \left(x_{\imath 1}^{(\kappa)}, x_{\imath 2}^{(\kappa)}, x_{\imath 3}^{(\kappa)}\right)^T \in \mathbb{R}^3$*, and* $z_\imath^{(\kappa)} = \left(z_{\imath 1}^{(\kappa)}, z_{\imath 2}^{(\kappa)}\right)^T \in \mathbb{R}^2$, $\bar{a} = 0.02, \bar{b} = 0.01$.

The other parameters are given as follows:

$$L^{(1)} = \begin{pmatrix} 2 & -1 & -1 \\ -1 & 1 & 0 \\ -1 & 0 & 1 \end{pmatrix}, L^{(2)} = \begin{pmatrix} 1 & 0 & -1 \\ 0 & 1 & -1 \\ -1 & -1 & 2 \end{pmatrix}, L^{(3)} = \begin{pmatrix} 2 & -1 & -1 \\ -1 & 2 & -1 \\ -1 & -1 & 2 \end{pmatrix},$$

$$H = \begin{pmatrix} 1 & 0.1 \\ 0 & 1 \\ 0 & 1 \end{pmatrix}, P = \begin{pmatrix} 1 & 0.1 \\ 0 & 1 \\ 0 & 1 \end{pmatrix}, D = \begin{pmatrix} 1 & -1 & 0 \\ -1 & 2 & -1 \\ 0 & -1 & 1 \end{pmatrix}, \Gamma = \begin{pmatrix} 1 & 1 & 0 \\ 0 & 1 & 1 \end{pmatrix}.$$

For our numerical simulation, we impose Adaptive Control Strategy (4) on FOOCMN (1) and choose the control parameters $\beta_\imath^{(\kappa)} \in [1, 1.2]$ *and* $g_\imath^\kappa(0) \in [0, 0.1]$, $\imath \in \tilde{\mathfrak{M}}$, $\kappa \in \tilde{\mathfrak{N}}$. *The corresponding simulation results are depicted in Figures 5–7, which demonstrate that the asymptotical synchronization of FOCMN (1) can be achieved.*

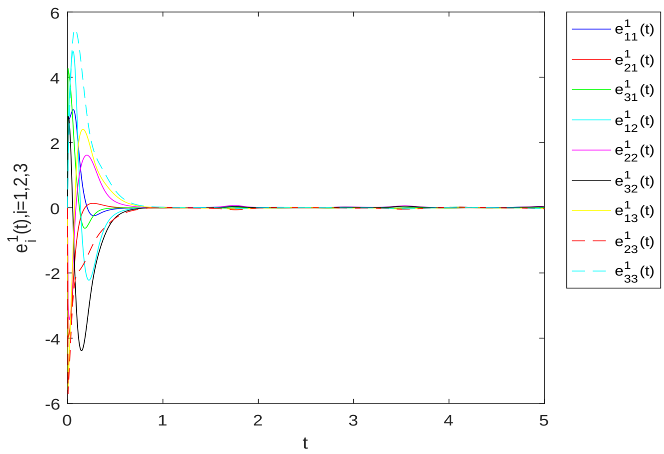

Figure 5. Synchronization error in the first layer under Controller (4).

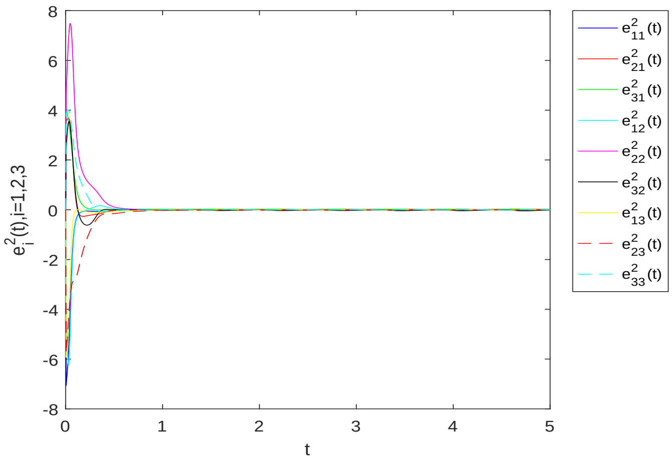

Figure 6. Synchronization error in the second layer under Controller (4).

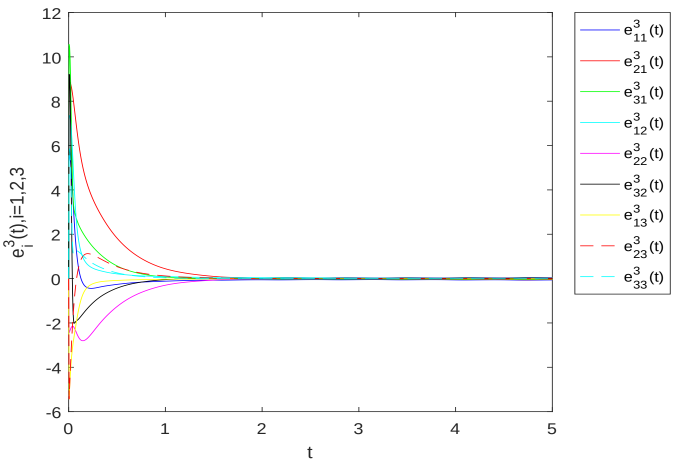

Figure 7. Synchronization error in the third layer under Controller (4).

Figure 8 shows the trajectories of the control gain function $g_\iota^{(\kappa)}(t)$, and it is easy to observe that they tend to be some numbers when System (1) achieves synchronization. From Figures 9–11, it can be seen nodes' dynamics are consistent with the target states under Controller (4). Figures 12 and 13 show the correctness of Remark 1 and Remark 2, respectively.

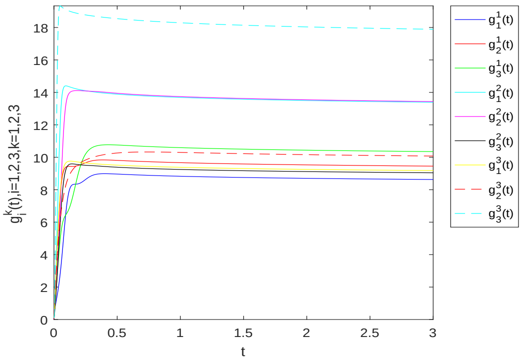

Figure 8. Evolutions of control gains $g_\iota^{(\kappa)}(t)$ under Controller (4).

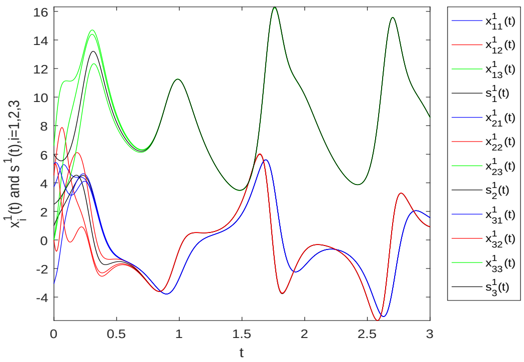

Figure 9. Trajectories of $x_\iota^{(1)}(t)$ and $s^{(1)}(t)$ under Controller (4).

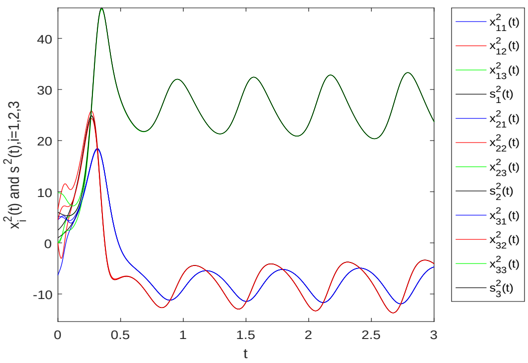

Figure 10. Trajectories of $x_\iota^{(2)}(t)$ and $s^{(2)}(t)$ under Controller (4).

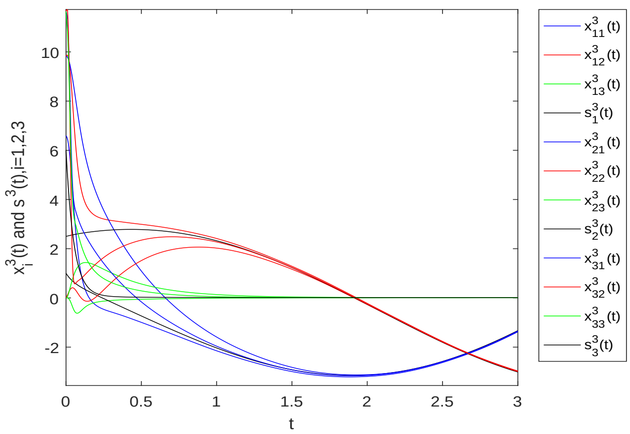

Figure 11. Trajectories of $x_i^{(3)}(t)$ and $s^{(3)}(t)$ under Controller (4).

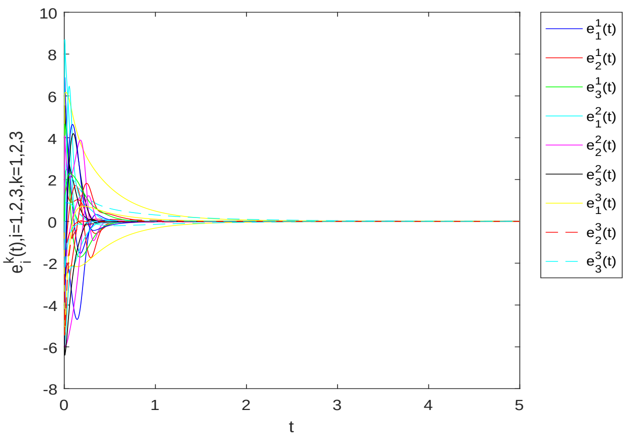

Figure 12. Synchronization error without inter-layer couplings under Controller (4).

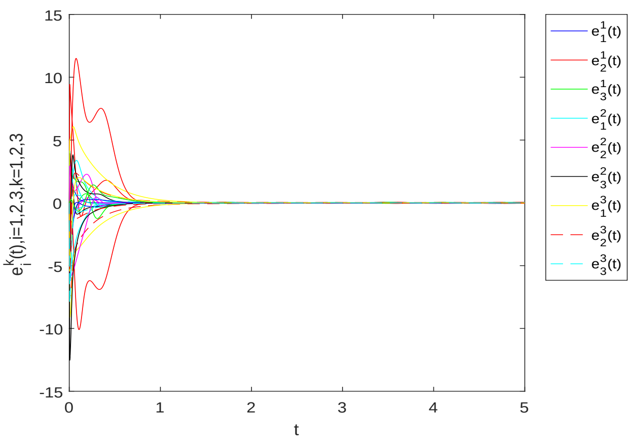

Figure 13. Synchronization error without intra-layer couplings under Controller (4).

Example 2. *Consider Adaptive Quantized Control Strategy (17) on FOOCMN (1) and choose $\xi_0 = 1$, $\rho = 0.3$; the other parameters are same as Example 1. The simulation results are depicted in Figures 14–19, and the varying control gains $\bar{g}_i^{(k)}(t)$ are shown in Figure 20.*

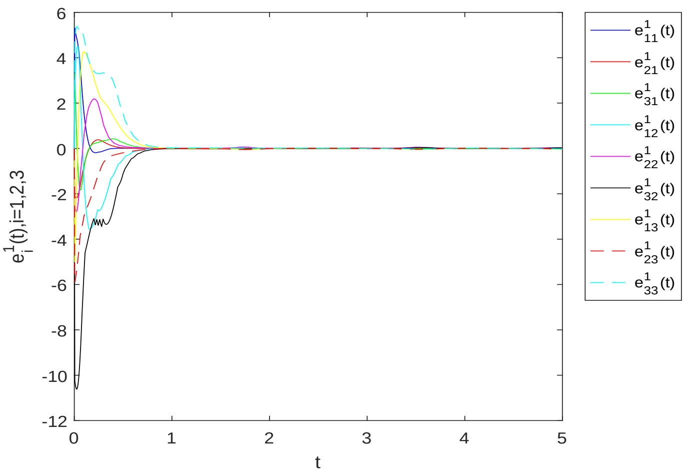

Figure 14. Synchronization error in the first layer under Controller (17).

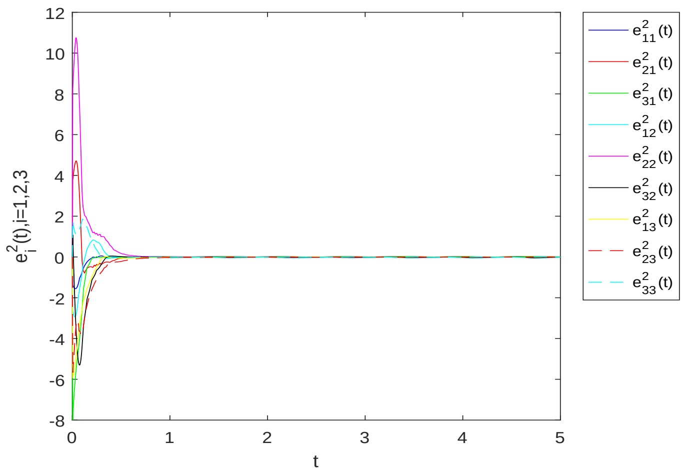

Figure 15. Synchronization error in the second layer under Controller (17).

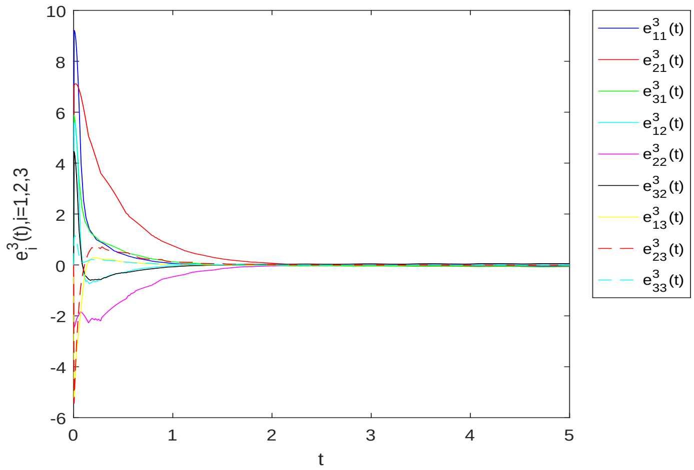

Figure 16. Synchronization error in the third layer under Controller (17).

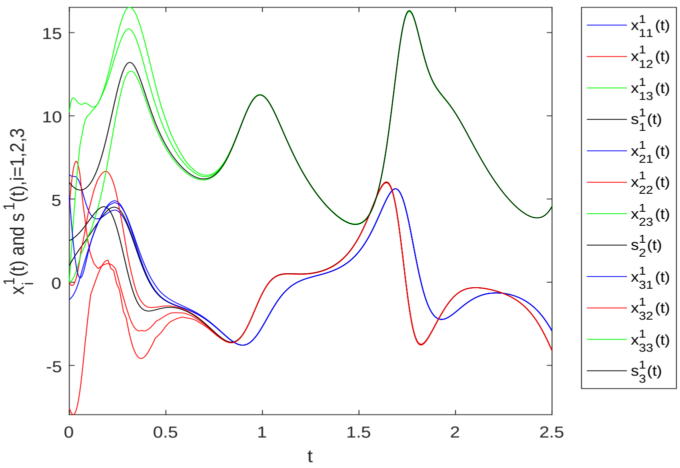

Figure 17. Trajectories of $x_i^{(1)}(t)$ and $s^{(1)}(t)$ under Controller (17).

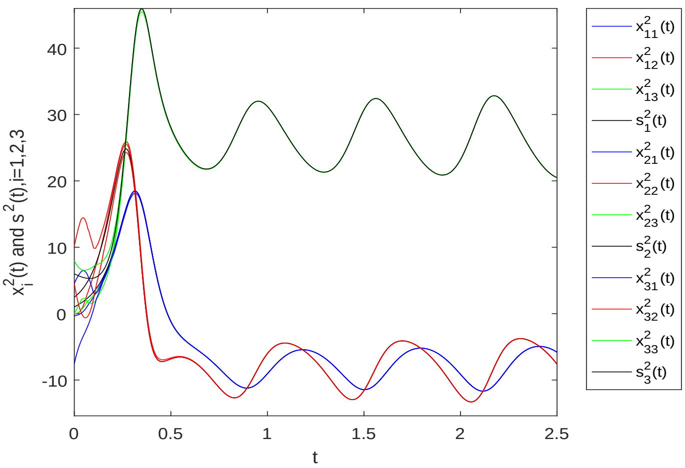

Figure 18. Trajectories of $x_i^{(2)}(t)$ and $s^{(2)}(t)$ under Controller (17).

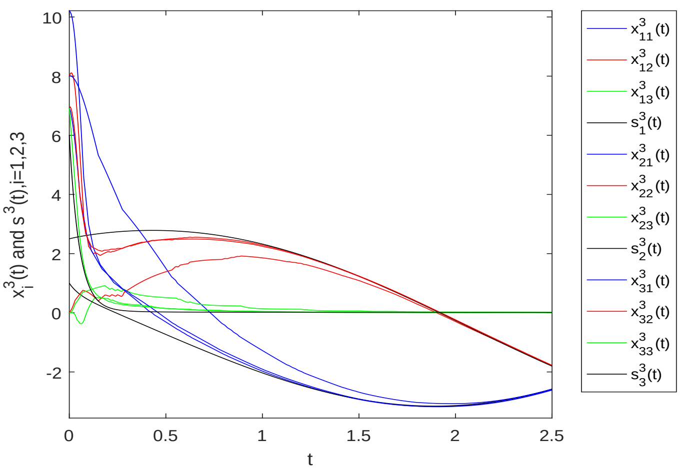

Figure 19. Trajectories of $x_i^{(3)}(t)$ and $s^{(3)}(t)$ under Controller (17).

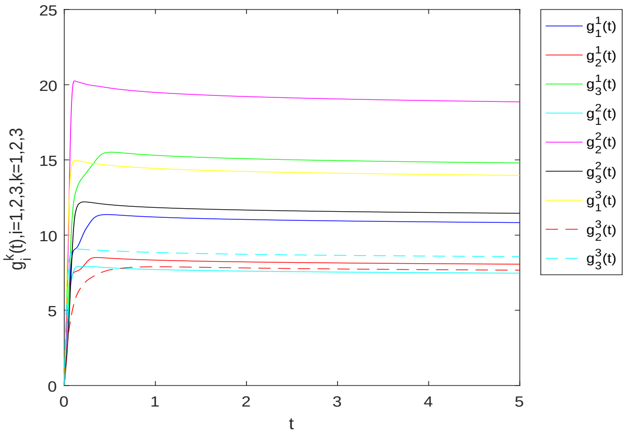

Figure 20. Evolutions of control gains $\bar{g}_\iota^{(\kappa)}(t)$ under Controller (17).

Figures 21–23 show the adaptive quantized controller $\bar{u}_\iota^{(\kappa)}(t)$ $(\iota \in \tilde{\mathfrak{M}}, \kappa \in \tilde{\mathfrak{N}})$ in each layer. Obviously, the continuous signals are translated as piecewise continuous forms via Quantized Controller (17), and the communication burden and the control cost are greatly reduced. Figures 24 and 25 show the correctness of Remark 5.

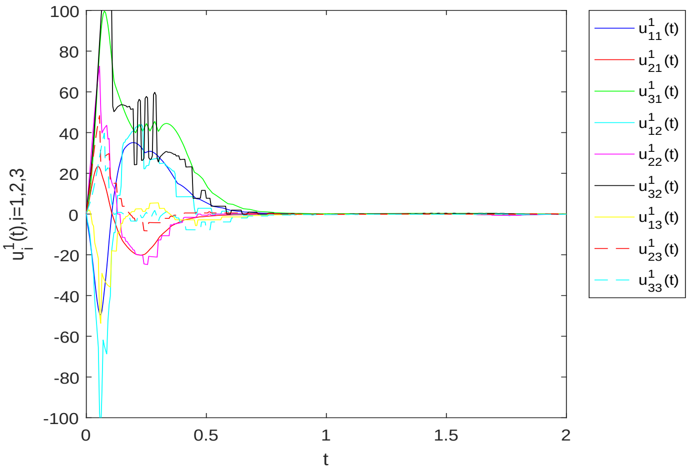

Figure 21. Quantized controller $\bar{u}_\iota^{(1)}(t)$ in the first layer.

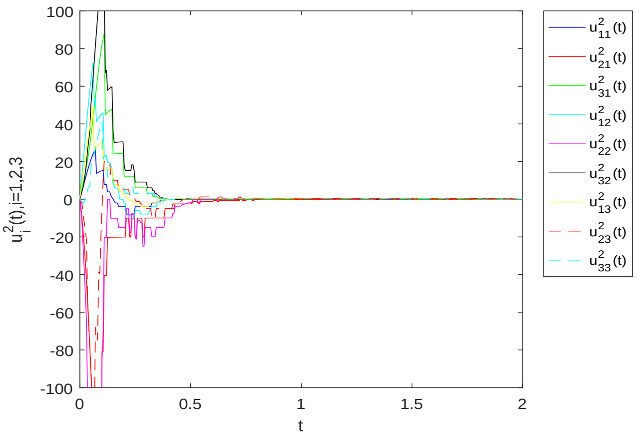

Figure 22. Quantized controller $\bar{u}_\iota^{(2)}(t)$ in the second layer.

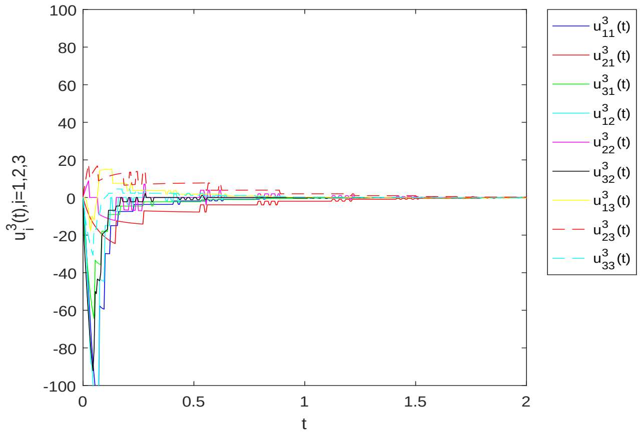

Figure 23. Quantized controller $\bar{u}_i^{(3)}(t)$ in the third layer.

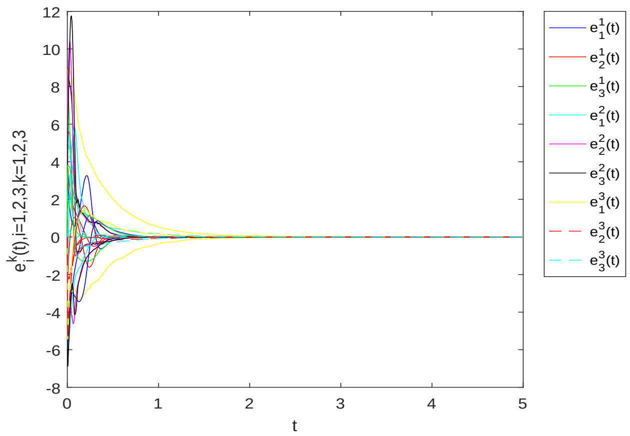

Figure 24. Synchronization error without inter-layer couplings under Controller (17).

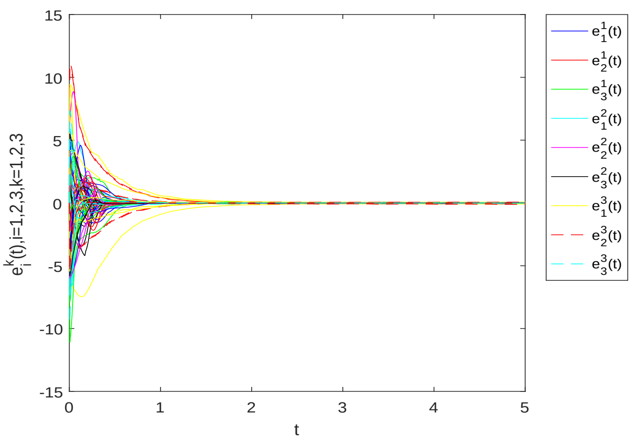

Figure 25. Synchronization error without intra-layer couplings under Controller (17).

As pointed out in Remarks 1, 2, and 5, the designed controllers and the synchronization criteria are applicable for the fractional-order multiplex networks without intra-layer coupling and inter-layer coupling. To validate this statement, Figures 12, 13, 24, and 25 are provided. It can be seen that the degraded multiplex networks without inter-layer coupling or intra-layer coupling require less synchronization time compared with the networks containing inter-layer and intra-layer coupling.

5. Conclusions

This paper investigated the synchronization problem of fractional-order output-coupling multiplex networks. Firstly, in the modelling of fractional-order multiplex networks, both intra-layer communication and inter-layer communication were considered based on nodes' dynamic outputs. Secondly, two kinds of adaptive control schemes were developed to realize the asymptotic synchronization of FOOCMNs. Note that the synchronized state of each layer is different, which is distinguished from the existing results. The developed control schemes and the synchronization criteria in this paper are more generic since they are also applicable when the fractional-order system is reduced to the integer-order multiplex model. Finally, several numerical examples were given to verify the theoretical analysis.

It is well known that the time delay is inevitable for large-scale complex networks in view of the limited information transmission and processing speed among nodes [30,47,48], so further research work would try to study the synchronization of FOOCMNs with time delays. Meanwhile, it is also interesting to reveal the effects of the number of layers on the synchronization of FOOCMNs, which will be considered in our latest research.

Author Contributions: Conceptualization, formal analysis, writing—original draft preparation, software, Y.B.; supervision, funding acquisition, validation, J.Y.; methodology, funding acquisition, writing—review and editing, C.H. All authors have read and agreed to the published version of the manuscript.

Funding: This work was supported by the National Natural Science Foundation of China (62263029, 61866036, 61963033), by the Key Project of Natural Science Foundation of Xinjiang (2021D01D10), by the Special Project for Local Science and Technology Development Guided by the Central Government (ZYYD2022A05) and by the Xinjiang Key Laboratory of Applied Mathematics (XJDX1401).

Data Availability Statement: Not applicable.

Acknowledgments: The authors are thankful to the handling editor and reviewers for their valuable comments and suggestions.

Conflicts of Interest: The authors declare no conflict of interest.

References

1. Gan, C.; Yang, X.; Liu, W. Propagation of computer virus both across the internet and external computers: a complex-network approach. *Commun. Nonlinear Sci. Numer. Simul.* **2014**, *19*, 2785–2792. [CrossRef]
2. Teeter, J.; Jacobs, A.; Werblin, F. How neural interactions form neural responses in the salamander retina. *J. Comput. Neurosci.* **1997**, *4*, 5–27. [CrossRef] [PubMed]
3. Barabási, A.; Albert, R. Emergence of scaling in random networks. *Science* **1999**, *286*, 509–512. [CrossRef] [PubMed]
4. Jin, X.; Wang, Z.; Chen, X.; Cao, Y.; Jiang, G. Stochastic synchronization of multiplex networks with continuous and impulsive couplings. *IEEE Trans. Netw. Sci. Eng.* **2021**, *8*, 2533–2544. [CrossRef]
5. Saha, S. Resilience in multiplex networks by addition of cross-repulsive links. *IEEE Trans. Netw. Sci. Eng.* **2022**, *9*, 1594–1603. [CrossRef]
6. Boccaletti, S.; Bianconi, G.; Criado, R. The structure and dynamics of multilayer networks. *Phys. Rep.* **2014**, *544*, 1–122. [CrossRef]
7. Mei, G.; Wu, X.; Wang, Y.; Hu, M.; Lu, J.; Chen, G. Compressive-sensing-based structure identification for multilayer networks. *IEEE Trans. Cybern.* **2018**, *48*, 754–764. [CrossRef]
8. D'Agostino, G.; Scala, A. *Networks of Networks: The Last Frontier of Complexity*; Elsevier: Amsterdam, The Netherlands; Springer International Publishing: Cham, Switzerland, 2014.
9. Chang, X.; Zhou, L.; Hu, F. Scale-free analysis of scientific collaboration hyper-networks. In Proceedings of the 2020 International Conference on Computer Science and Management Technology, Shanghai, China, 20–22 November 2020; pp. 85–90.
10. Kumar, R.; Narayan, S.; Kumar, S.; Roy, S. Knowledge-based neural networks for fast design space exploration of hybrid copper-graphene on-chip interconnect networks. *IEEE Trans. Electromagn. Compat.* **2021**, *99*, 1–14. [CrossRef]
11. Amato, R.; Diaz-Guilera, A.; Kleineberg, K. Interplay between social influence and competitive strategical games in multiplex networks. *Sci. Rep.* **2017**, *7*, 7087–7087. [CrossRef]
12. Nicosia, V.; Latora, V. Measuring and modeling correlations in multiplex networks. *Phys. Rev. E* **2015**, *92*, 032805. [CrossRef]
13. Pocock, M.; Evans, D.; Memmott, J. The robustness and restoration of a network of ecological networks. *Science* **2012**, *335*, 973–977. [CrossRef]

14. Chen, L.; Wu, R.; Cheng, Y.; Chen, Y. Delay-dependent and order-dependent stability and stabilization of fractional-order linear systems with time-varying delay. *IEEE Trans. Circuits Syst. II Express Briefs* **2020**, *67*, 1064–1068. [CrossRef]
15. Fu, H.; Wu, G.; Yang, G.; Huang, L. Fractional calculus with exponential memory. *Chaos, Solitons Fractals* **2021**, *31*, 031103. [CrossRef]
16. Hong, L.; Cao, J.; Jiang, H.; Alsaedi, A. Graph theory-based finite-time synchronization of fractional-order complex dynamical networks. *J. Frankl. Inst.* **2018**, *355*, 5771–5789.
17. Yang, S.; Yu, J.; Hu, C.; Jiang, H. Finite-time synchronization of memristive neural networks with fractional-order. *IEEE Trans. Syst. Man, Cybern. Syst.* **2021**, *51*, 3739–3750. [CrossRef]
18. Wu, G.; Abdeljawad, T.; Liu, J.; Baleanu, D.; Wu, K. Mittag-leffler stability analysis of fractional discrete-time neural networks via fixed point technique. *Nonlinear Anal. Model. Control.* **2019**, *24*, 919–936. [CrossRef]
19. Chen, C.; Zhu, S.; Wei, Y.; Chen, C. Finite-time stability of delayed memristor-based fractional-order neural networks. *IEEE Trans. Cybern.* **2020**, *50*, 1607–1616. [CrossRef]
20. Yang, S.; Yu, J.; Hu, C.; Jiang, H. Exponential stability of fractional-order impulsive control systems with applications in synchronization. *IEEE Trans. Cybern.* **2020**, *50*, 3157–3168. [CrossRef]
21. Wu, X.; Bao, H. Finite time complete synchronization for fractional-order multiplex networks. *Appl. Math. Comput.* **2020**, *377*, 125188. [CrossRef]
22. Li , C.; Liao, X.; Wong, K. Lag synchronization of hyperchaos with application to secure communications. *Chaos Solitons Fractals* **2005**, *23*, 183–193. [CrossRef]
23. Sun, K.; Liu, L.; Qiu, J.; Feng, G. Fuzzy adaptive finite-time fault-tolerant control for strict-feedback nonlinear systems. *IEEE Trans. Fuzzy Syst.* **2021**, *29*, 786-796. [CrossRef]
24. Xu, Y.; Gao, S.; Li, W. Exponential stability of fractional-order complex multi-links networks with aperiodically intermittent control. *IEEE Trans. Neural Netw. Learn. Syst.* **2021**, *32*, 4063–4074. [CrossRef] [PubMed]
25. Zhang, N.; Chen, H.; Li, W. Stability for multi-links stochastic delayed complex networks with semi-markov jump under hybrid multi-delay impulsive control. *Neurocomputing* **2021**, *449*, 214-228. [CrossRef]
26. Wang, S.; Cao, Y. ; Guo, Z.; Yan, Z.; Huang, T. Periodic event-triggered synchronization of multiple memristive neural networks with switching topologies and parameter mismatch. *IEEE Trans. Cybern.* **2021**, *51*, 427–437. [CrossRef] [PubMed]
27. Lv, Y.; Hu, C.; Yu, J.; Jiang, H.; Huang, T. Edge-based fractional-order adaptive strategies for synchronization of fractional-order coupled networks with reaction-diffusion terms. *IEEE Trans. Cybern.* **2018**, *50*, 1582–1594. [CrossRef]
28. Yang, Y.; Hu, C.; Yu, J.; Jiang, H.; Wen, S. Synchronization of fractional-order spatiotemporal complex networks with boundary communication. *Neurocomputing* **2021**, *450*, 197–207. [CrossRef]
29. Liu, P.; Xu, M.; Sun, J.; Zeng, Z. On pinning linear and adaptive synchronization of multiple fractional-order neural networks with unbounded time-varying delays. *IEEE Trans. Cybern.* **2022**. [CrossRef]
30. Luo, T.; Wang, Q.; Jia, Q.; Xu, Y. Asymptotic and finite-time synchronization of fractional-order multiplex networks with time delays by adaptive and impulsive control. *Neurocomputing* **2022**, *493*, 445–461. [CrossRef]
31. Kalman, R. Nonlinear aspects of sampled-data control systems. *Proc. 1956 Symp. Nonlinear Circuit Anal.* **1956**, *6*, 273–313.
32. Wu, Z.; Xu, Y.; Pan, Y.; Su, H.; Tang, Y. Event-triggered control for consensus problem in multi-agent systems with quantized relative state measurements and external disturbance. *IEEE Trans. Circuits Syst. Regul. Pap.* **2018**, *65*, 2232–2242. [CrossRef]
33. Sun, B.; Cao, Y.; Guo, Z.; Yan, Z.; Wen, S. Synchronization of discrete-time recurrent neural networks with time-varying delays via quantized sliding mode control. *Appl. Math. Comput.* **2020**, *375*, 125093. [CrossRef]
34. Bao, H.; Park, J.; Cao, J. Adaptive synchronization of fractional-order output-coupling neural networks via quantized output control. *IEEE Trans. Neural Netw. Learn. Syst.* **2021**, *32*, 3230–3239. [CrossRef]
35. Zhuang, J.; Cao, J.; Tang, L.; Xia, Y.; Perc, M. Synchronization analysis for stochastic delayed multilayer network with additive couplings. *IEEE Trans. Syst. Man, Cybern. Syst.* **2020**, *50*, 4807–4816. [CrossRef]
36. Wang, Z.; Jin, X.; Pan, L.; Feng, Y.; Cao, J. Quasi-synchronization of delayed stochastic multiplex networks via impulsive pinning control. *IEEE Trans. Syst. Man, Cybern. Syst.* **2022**, *52*, 5389–5397. [CrossRef]
37. Jin, X.; Wang, Z.; Yang, H.; Song, Q.; Xiao, M. Synchronization of multiplex networks with stochastic perturbations via pinning adaptive control. *J. Frankl. Inst.* **2021**, *358*, 3994–4012. [CrossRef]
38. Kilbas, A.; Srivastava, H.; Trujillo, J. Theory and applications of fractional differential equations. *North-Holl. Math. Stud.* **2006**, *204*, 1–523.
39. Aguila, N.; Duarte, M.; Gallegos, J. Lyapunov functions for fractional order systems. *Commun. Nonlinear Sci. Numer. Simul.* **2014**, *19*, 2951–2957. [CrossRef]
40. Li, W.; Zhou, J.; Li, J.; Xie, T.; Lu, J. Cluster synchronization of two-layer networks via aperiodically intermittent pinning control. *IEEE Trans. Circuits Syst. II Express Briefs* **2021**, *68*, 1338–1342. [CrossRef]
41. Xu, Y.; Wu, X.; Mao, B.; Lu, J.; Xie, C. Finite-time intra-layer and inter-layer quasi-synchronization of two-layer multi-weighted networks. *IEEE Trans. Circuits Syst. Regul. Pap.* **2021**, *68*, 1589–1598. [CrossRef]
42. Liu, H.; Li, J.; Li, Z.; Zeng, Z.; Lu, J. Intralayer synchronization of multiplex dynamical networks via pinning impulsive control. *IEEE Trans. Cybern.* **2022**, *52*, 2110–2122. [CrossRef]
43. Pecora, L.; Sorrentino, F.; Hagerstrom, A.; Murphy, T.; Roy, R. Cluster synchronization and isolated desynchronization in complex networks with symmetries. *Nat. Commun.* **2014**, *5*, 4079. [CrossRef] [PubMed]

44. Tang, Z.; Park, J.; Wang, Y.; Zheng, W. Synchronization on lur'e cluster networks with proportional delay: impulsive effects method. *IEEE Trans. Syst. Man, Cybern. Syst.* **2021**, *51*, 4555–4565. [CrossRef]
45. Hu, C.; Jiang, H. Pinning synchronization for directed networks with node balance via adaptive intermittent control. *Nonlinear Dyn.* **2015**, *80*, 295–307. [CrossRef]
46. Wu, Y.; Liu, L.; Hu, J.; Feng, G. Adaptive antisynchronization of multilayer reaction-diffusion neural networks. *IEEE Trans. Neural Netw. Learn. Syst.* **2018**, *29*, 807–818. [CrossRef]
47. Liu, P.; Kong, M.; Zeng, Z. Projective synchronization analysis of fractional-order neural networks with mixed time delays. *IEEE Trans. Cybern.* **2020**. [CrossRef]
48. Liu, P.; Xu, M.; Sun, J.; Wen, S. Cluster synchronization of multiple fractional-order recurrent neural networks with time-varying delays. *IEEE Trans. Neural Netw. Learn. Syst.* **2021**. [CrossRef]